Nucleation in periodically driven electrochemical systems

V. N. Smelyanskiy
Caelum Research Corporation, NASA Ames Research Center, MS 269-2, Moffet Field, California 94035-1000

M. I. Dykman
Department of Physics and Astronomy, Michigan State University, East Lansing, Michigan 48824

H. Rabitz, B. E. Vugmeister, S. L. Bernasek, and A. B. Bocarsly
Department of Chemistry, Princeton University, Princeton, New Jersey 08544

(Received 18 November 1998; accepted 5 March 1999)

We calculate both the exponent and the prefactor in the nucleation rate of a periodically driven system. Nucleation dynamics is described by the Fokker–Planck equation for the probability distribution of the nuclei over their size. This distribution is found using the concept of the most probable (optimal) nucleation path. The results apply in a broad range of driving force amplitudes, from weak to moderately strong forces where the nucleation rate is changed exponentially strongly, and also in the broad range of the driving frequencies, from low-frequency driving, where the system follows the force adiabatically, to high-frequency nonadiabatic driving. For strong driving forces, the time dependence of the nucleation rate changes from strongly nonsinusoidal to a weak with the increasing frequency of driving. The response of the nucleation rate to the driving force is described in terms of logarithmic susceptibility (LS), which can be obtained from the optimal nucleation path in the absence of the driving. LS is a smooth function of frequency, and therefore even a driving force with comparatively high frequency can change the modulation rate exponentially strongly. LS and the Faraday current are calculated for simple models of electrochemical systems, where the ac driving is produced by modulation of the electrode potential. We also suggest how to find LS from measurements of the average nucleation rate. © *1999 American Institute of Physics.* [S0021-9606(99)50121-9]

I. INTRODUCTION

The initial stage of electrochemical growth is often nucleation of a sufficiently large atomic cluster of deposited metal (a critical nucleus), which then spontaneously grow. Nucleation occurs via fluctuational attachment of atoms to the growing nucleus accompanied, in case of overpotential deposition, by electric discharge of metal ions on the metal surface.

A simple theoretical approach to nucleation is based on the assumption that the state of the nucleus is fully characterized by the number of atoms in it, g. This approach has been broadly used in literature[1–6] and has been demonstrated to account for many qualitative features of the nucleation process in various physical systems.

In quasi-equilibrium conditions, at constant pressure and temperature, growth of a nucleus of size g is determined by its Gibbs free energy $\Phi_0(g)$. In general, $\Phi_0(g)$ can be written in the form

$$\Phi_0 = -\delta\mu_0 g + A(g), \tag{1}$$

where the first term is the volume energy and the second term is the surface energy of the nucleus. The deviation $\delta\mu_0$ ($\delta\mu_0 > 0$) of the chemical potential from its equilibrium value is determined by the deviation η_0 of the actual electrode potential from the Nernstian equilibrium potential, $\delta\mu_0 = |Ze\,\eta_0|$, where $-Ze$ is the charge of cations in electrolyte. The value of $\delta\mu_0$ determines the driving force in the system and controls the size of a critical nucleus g^*. In what follows we call $\delta\mu_0$ supersaturation.

For nuclei of a subcritical size, $g < g^*$, the free energy $\Phi_0(g)$ increases with increasing g. The size g^* of the critical nucleus corresponds to the maximum of $\Phi_0(g)$. The supercritical nuclei with $g > g^*$ grow spontaneously. The quantity $\Phi_0^* = \Phi(g^*)$ is the activation energy for nucleation.

In this paper we will analyze the problem of nucleation in systems driven by a time-periodic force. The results will be applied to nucleation in electrodeposition for an ac potential. Analysis of the effects of ac driving on electrochemical deposition has been done so far for weak ac potentials, in which case the quantity of interest was the impedance of the electric double layer between the electrode surface and the electrolyte.[7] Some results have also been obtained on the effects of very strong ac driving forces where there arise spatially nonuniform macroscopic flows, as in convection-limited growth[8] and ultrasonically induced cavitation.[9]

We will consider the case where the ac driving force is relatively weak, so that it does not give rise to spatially nonuniform macroscopic flows, yet it modulates the nucleation barrier and thus may very strongly change the nucleation rate. The effect of barrier modulation is very general and is not limited to electrochemical systems.[10] However, electrochemical systems are advantageous for analysis of this effect, since the ac driving force can be easily produced by varying the electrode potential. There is experimental evidence[11] that the nucleation rate in an electrochemical sys-

tem may indeed be strongly changed by a relatively weak ac driving.

We will assume that the ac driving force is sufficiently slow as compared to the RC time of the electric double layer. Yet the period of force $T=2\pi/\omega$ may still be comparable to the characteristic decay time τ^* of a subcritical nucleus. Time τ^* describes the collective motion of $g\sim g^*\gg 1$ atoms, and therefore it largely exceeds the characteristic dynamical times of individual atoms, like the period of atomic vibrations ($\sim 10^{-13}\div 10^{-14}$ s). In this case the attachment/detachment rates for individual atoms satisfy the detailed balance condition, and the free energy of the cluster $\Phi(g,t)$ follows the driving force *adiabatically*, i.e., without a time lag, as also does the cluster size distribution. However, for the driving force frequencies $\omega\gtrsim 1/\tau^*$ one may not think of the nucleation rate as the rate for a given $\Phi(g,t)$, since retardation of the collective motion of nucleating monomers becomes substantial.

The expression for $\Phi(g,t)$ in an ac driven system is formally given by Eq. (1) in which $\delta\mu=\delta\mu(t)$ is the instantaneous chemical potential of the adatoms on the surface counted off from the equilibrium value,

$$\delta\mu(t)=\delta\mu_0+h(t),\quad h(t)=\sum_{n\neq 0} h_n\exp(i\omega nt). \tag{2}$$

Here, h_n are complex amplitudes of the Fourier harmonics of the periodic driving force $h(t)$. We assume that $h(t)$ has no time-independent component, $h_0=0$.

For sufficiently low supersaturation, where $|\delta\mu_0|\ll kT$, and for large critical nucleus. $g^*\gg 1$, nucleation kinetics can be described by the Fokker–Planck equation (FPE) for the distribution function $f(g,t)$ of the nuclei over their size g,

$$\frac{\partial f}{\partial t}=-\frac{\partial j}{\partial g}, \tag{3}$$

with the flux $j(g,t)$ given by

$$j=-a(g)\left(\frac{\partial\Phi}{\partial g}f(g,t)+D\frac{\partial f(g,t)}{\partial g}\right),\quad D=k_BT. \tag{4}$$

Here, $Da(g)$ is the rate of attachment of monomers to the nucleus of size g, and it corresponds to the diffusion coefficient in g-space.

In the steady state, $\Phi(g,t)\equiv\Phi_0(g)$ is time independent; then Eqs. (3) and (4) go over into the familiar Zeldovich–Frenkel equation of the classical nucleation theory.[1] In Ref. 1, the steady-state distribution of subcritical nuclei is close to the Gibbs distribution,

$$\begin{aligned} &f_0(g)=n_0\exp[-\Phi_0(g)/D],\\ &\Phi_0^*-\Phi_0(g)\gg D,\quad \Phi_0^*=\Phi_0(g^*), \end{aligned} \tag{5}$$

where n_0 is the number density of free monomers.

On the other hand, the distribution in the critical and supercritical regions is strongly nonequilibrium and corresponds to a constant flux $j(g)=\mathcal{J}_0$ over the free-energy barrier. For supercritical nuclei away from the critical region, the diffusion component of flux Eq. (4) can be neglected, and the steady-state distribution has the form

$$\begin{aligned} &f_0(g)=-\frac{\mathcal{J}_0}{a(g)}\frac{1}{d\Phi_0/dg},\quad |g-g^*|\gg(D\beta^*)^{1/2},\\ &\beta^*=-1/\Phi_0''(g_0^*),\quad \Phi''\equiv d^2\Phi/dg^2. \end{aligned} \tag{6}$$

Flux $\mathcal{J}_0$ is equal to the rate of production of sufficiently large supercritical nuclei which most likely will not collapse, i.e., to the nucleation rate. The value of $\mathcal{J}_0$ is given by the activation law (cf. Refs. 1–3)

$$\begin{aligned} &\mathcal{J}_0=B_0\exp[-\Phi_0^*/D],\quad \Phi_0^*\gg D,\\ &B_0=n_0a(g^*)(2\pi\beta^*D)^{-1/2}, \end{aligned} \tag{7}$$

where β^* is defined in Eq. (6). Expression (7) is the central result of the classical droplet theory of nucleation which was obtained in Ref. 1(a) (see also Refs. 2 and 3 for details) as an application of the Kramers theory of escape rates.[12]

For periodically driven systems, after transient time the distribution function $f(g,t)$ depends on time periodically, with the period of the driving, and so does the steady-state nucleation rate. For a sufficiently large driving force the variation in time of $\Phi(g,t)$ can exceed D; then the effect of the driving force on the distribution function and nucleation rate will be *exponentially* strong. Unlike the stationary case, flux $j(g,t)$ periodically depends on time; it also depends on the size of the nuclei. This dependence is well understood in the limit of low frequencies of the driving force where the system adiabatically follows the force, and the nucleation rate is described by the Frenkel–Zeldovich theory with $\delta\mu_0$ replaced by the instantaneous $\delta\mu(t)$. A step toward analysis of the effect of nonadiabatic driving was made in Ref. 13 for a specific model where $\Phi(g)$ is an infinite parabolic barrier, and atoms are ''injected'' at some g at a constant rate.

In what follows we provide a general explicit solution of the problem of the nucleation rate in ac driven electrochemical systems, including both the exponent and the prefactor. The solution describes the nucleation rate and Faraday current in a broad range of driving force frequency ω. We consider a steady regime where the nucleation rate is periodic in time with period $2\pi/\omega$. Aperiodic transients decay within the characteristic relaxation time τ^*, which is closely related to the induction time previously studied in transient nucleation with constant supersaturation.[5]

In Sec. II we formulate the problem and relate the nucleation rate in a periodically driven system to the current in the supercritical region. In Sec. III we derive the expression for the nucleation rate to logarithmic accuracy (calculate the effective activation energy of nucleation) in the case of a high-frequency (nonadiabatic) driving force using the WKB-type approach to the FPE. In Sec. IV A we calculate explicitly the exponential factor in the nucleation rate in the case where the driving force is not very strong, and yet it affects the nucleation rate exponentially strongly. We show that this occurs in a broad range of amplitudes of the ac driving force where the variation of the logarithm of the nucleation rate is simply *linear* in the driving force and therefore can be described by *logarithmic susceptibility* (LS). In Sec. IV B we obtain the explicit expression for the nucleation rate, including the prefactor, in the cases of nonadiabatic and adiabatic driving, and analyze the crossover between the two regimes. In Sec. V we

calculate LS for several nucleation models relevant to 2D nucleation in electrochemical deposition. We also analyze how spectral properties of LS affect the nucleation rate and suggest a simple method of experimental analysis of LS. In Sec. VI we calculate the Faraday current for several models of electrochemical nucleation. Section VII contains concluding remarks.

II. NUCLEATION RATE: GENERAL FORMULATION

We start with the analysis of the nucleus dynamics in the neglect of fluctuations. In this case, time variation of the size of nuclei $g(t)$ is described by the drift term in the FPE (3) and (4). Using the explicit form of Φ in Eqs. (1) and (2), we obtain

$$\dot{g}(t)=K(g,t), \quad K=a(g)\left[\delta\mu(t)-\frac{\partial A}{\partial g}\right]. \tag{8}$$

This equation has an unstable periodic solution:

$$g^*(t)=g^*(t+T). \tag{9}$$

If at time t a nucleus has a size $g<g^*(t)$, it will collapse, whereas if $g>g^*(t)$, it will grow. Thus $g^*(t)$ corresponds to a time-dependent size of the critical nucleus. In the limit of weak driving amplitude, $|h(t)/\delta\mu_0|\ll 1$, the value of $g^*(t)$ is close to critical size for the undriven system.

In the presence of fluctuations, a nucleus with $g<g^*(t)$ can grow, in which case the fluctuation works against the drift force $K(g,t)$. To do this the fluctuation has to be sufficiently large. However, once the nearly critical size is reached, $|g-g^*(t)|\sim(D\beta^*)^{1/2}$, the drift force becomes small, and the dynamics of nuclei is determined by small fluctuations. With probability $\sim 1/2$ the nucleus can go onto either side of $g^*(t)$. As a result, it will either collapse or grow. For the nuclei that at some instant t reach a supercritical size $g-g^*(t)\gg(D\beta^*)^{1/2}$, the diffusion component of the flux in Eq. (4) becomes negligible and they will most likely increase in size following the deterministic growth law Eq. (8), i.e.,

$$j(g,t)\approx K(g,t)f(g,t), \quad g-g^*(t)\gg(D\beta^*)^{1/2}. \tag{10}$$

From Eq. (10), the instantaneous nucleation rate can be defined as the rate at which there emerge large enough supercritical nuclei. Consider at some time t the number density $n(z,t)$ of supercritical nuclei with sizes $g\geqslant g^*(t)+z$. We choose the offset z to be sufficiently large, so that it is unlikely that any of these nuclei will collapse. However, we will assume that z is small compared to the nonlinear scale of the problem given by critical size $g^*(t)$. We then define the rate of nucleation $\mathcal{J}(z,t)$ as

$$\begin{aligned}&\mathcal{J}(z,t)=\frac{\partial n(z,t)}{\partial t},\\ &n(z,t)=\int_{g^*(t)+z}^{\infty} dg f(g,t), \quad g^*\gg z\gg(D\beta^*)^{1/2}.\end{aligned} \tag{11}$$

It can be immediately seen from Eqs. (3), (4), and (11) that, for small z/g^*, one obtains

$$\mathcal{J}(z,t)\approx K_g^*(t)zf(g^*(t)+z,t),$$

$$K_g^*(t)=\frac{\partial K(g,t)}{\partial g} \text{ for } g=g^*(t). \tag{12}$$

To gain a better understanding of expression (12), we expand in FPE (3) the drift force $K(g,t)$ and $a(g)$ in the deviation from the critical state $z=g-g^*(t)$. In variables z,t, FPE takes the form

$$\begin{aligned}&\frac{\partial\tilde{f}(z,t)}{\partial t}=-\frac{\partial\tilde{j}(z,t)}{\partial z}, \quad \tilde{f}(z,t)=f(g^*(t)+z),\\ &\tilde{j}(z,t)=[zK_g^*-Da_g^*(t)]\tilde{f}(z,t)-Da^*(t)\frac{\partial\tilde{f}(z,t)}{\partial z}, \quad (13)\\ &a^*(t)=a(g^*(t)), \quad a_g^*=\frac{\partial a(g^*(t))}{\partial g^*}.\end{aligned}$$

For large enough z, the periodic flux $\tilde{j}(z,t)$ is given by the expression [cf. Eq. (10)]

$$\tilde{j}(z,t)=zK_g^*(t)\tilde{f}(z,t), \quad z\gg(D\beta^*)^{1/2}. \tag{14}$$

From Eqs. (14) and (12) we see that

$$\mathcal{J}(z,t)=\tilde{j}(z,t), \tag{15}$$

i.e., the nucleation rate is given by the periodic probability flux $\tilde{j}(z,t)$.

In the supercritical range $z\gg(D\beta^*)^{1/2}$ one can neglect the diffusion term in Eq. (13), and then the distribution function $\tilde{f}(z,t)$ can be calculated along the trajectories Eq. (8) of deterministic growth. These trajectories emanate at $t\to-\infty$ from the unstable state $z=0$. From Eq. (13) we obtain:

$$\begin{aligned}&\tilde{f}_s(z,t)\approx\frac{1}{z}\Pi(zu(t,0)),\\ &u(t,t')=\exp\left[-\int_{t'}^{t}K_g^*(\tau)d\tau\right],\end{aligned} \tag{16}$$

where $\Pi(x)$ is an arbitrary function. Substituting the above expression in Eq. (12), we obtain the steady-state nucleation rate in the form

$$\mathcal{J}(z,t)=K_g^*(t)\Pi(zu(t,0)). \tag{17}$$

The time dependence of the nucleation rate $\mathcal{J}(z,t)$ comes from the factor K_g^* and the function $\Pi(c)$. The latter function is constant along the deterministic growth paths $z(t,c)=cu^{-1}(t,0)$ given by Eq. (8), but it varies from path to path. We note that this function cannot be found just from the solution of Eq. (13) in the supercritical range; It is determined by the values of the distribution function at small $z\sim(D\beta^*)^{1/2}$ where the diffusion is important. To find it one has to match solution (16) in the supercritical region to the time-periodic distribution function obtained by the solution of FPE in the entire region $g\lesssim g^*(t)$.

The boundary condition to FPE (3) on the small-g side can be established by noticing that the time-dependent driving Eq. (2) affects the volume energy of the nucleus, but not its surface energy $A(g)$,

$$A(g)=\gamma g^{1-1/d}, \tag{18}$$

where γ is the effective surface tension and d is the dimension of the nucleus. For nuclei much smaller than the critical size $g^*(t)$ [more precisely, than the minimal value of $g^*(t)$ per period], the surface energy exceeds the volume energy, and the effect of ac driving is not important.

Therefore in the time-periodic regime the distribution of small nuclei is close to the Gibbs distribution Eq. (5),

$$f(g,t)=n_0\exp[-A(g)/D], \quad g\ll\min_t g^*(t). \tag{19}$$

irrespective of driving.

Nucleation rate averaged over the period of modulation

The distribution $f(g,t)$ depends on time periodically, and the left hand side of Eq. (3) equals zero after averaging over the period of the driving force. Therefore the time-averaged flux $j(g,t)$ is constant in steady state. Then, according to Eq. (11), the average nucleation rate $\overline{\mathcal{J}}$ just equals the average flux and does not depend on the choice of the boundary of the supercritical region,

$$\overline{\mathcal{J}}=\langle\mathcal{J}(z,t)\rangle=\langle\tilde{j}(z,t)\rangle=\text{const}, \tag{20}$$

where $\langle\cdots\rangle$ means averaging over the driving force period T.

We note that the z dependence of the instantaneous nucleation rate $\mathcal{J}(z,t)$ is due to the dependence on z of the duration of motion to $g^*(t)+z$ along the deterministic trajectory Eq. (8) from the vicinity of $g^*(t)$ (where the population periodically varies in time). Clearly, the z dependence disappears upon time averaging.

III. EXPONENT FOR THE NUCLEATION RATE AND THE DISTRIBUTION FUNCTION OF NUCLEI

A. The eikonal approximation. Optimal fluctuational paths

For small fluctuation intensities D, function $f(g,t)$ is concentrated mostly in the range of small nuclei size where $\Phi(g)\sim D\ll\Phi^*$. Distribution of the nuclei in the range where $\Phi(g)\gg D$ is formed by large fluctuations. In this range the tail of $f(g,t)$ is exponentially steep in g, for $g<g^*(t)$. To determine the distribution of large subcritical nuclei we will look for the solution of Eq. (3) in the form

$$f(g,t)=C(g,t)\exp[-R(g,t)/D], \quad R\gg D. \tag{21}$$

This form is analogous to the Gibbs distribution in equilibrium systems Eq. (6), with $R(g,t)$ being the ''activation energy'' of fluctuations to the state with the nucleus size g at the instant t. Equation (21) is similar to the eikonal approximation in optics or the WKB approach in quantum mechanics. This approach or the equivalent path-integral technique was applied to analysis of large fluctuations in noisy dynamical systems far from equilibrium, including stationary[14–19] and periodically driven systems.[10,20–23] It was also used in chemical kinetics.[24] The idea of the approach is that, as a first step, one should substitute Eq. (21) into FPE (3) and keep the terms of the leading order in D. This gives the following equation for $R(g,t)$:

$$\frac{\partial R}{\partial t}+H\left(g,\frac{\partial R}{\partial g},t\right)=0,$$
$$H(g,p,t)=K(g,t)p+a(g)p^2, \quad p\equiv\frac{\partial R}{\partial g}, \tag{22}$$

where $K(g,t)$ is defined in Eq. (8).

Equation (22) has the form of the Hamilton–Jacobi equation for an auxiliary mechanical system with coordinate g, momentum p, and Hamiltonian $H(g,p,t)$.[25] The activation energy $R(g,t)$ corresponds to the mechanical action of the auxiliary system.

The Hamilton-Jacobi Eq. (22) can be solved by the method of characteristics. The equations for the characteristics have the form

$$\dot{g}=\frac{\partial H}{\partial p}=K+2ap, \tag{23a}$$

$$\dot{p}=-\frac{\partial H}{\partial g}=-\frac{\partial K}{\partial g}p-\frac{\partial a}{\partial g}p^2, \tag{23b}$$

$$\dot{s}=\dot{g}p-H, \quad s(t)\equiv R(g(t),t). \tag{23c}$$

The physical meaning of the characteristics can be understood as follows. A nuclei of size g_f at the instant t_f has been formed as a result of a large fluctuation. Most probably, in this fluctuation the size of the nucleus was evolving in a way close to some optimal way which corresponds to g varying along the optimal fluctuational path $g(t)$, which arrives at g_f for $t=t_f$. It is this path that is described by Eq. (23). We note that the optimal path begins at some instant of time t_0 where $g(t_0)$ corresponds to a microscopic nucleus and in the continuous theory, is set equal to zero, $g=0$.

From boundary conditions (19) and Eq. (21) it follows that $R(g,t)\approx A(g)$ for small-g. Using this relation and Eqs. (22) and (23), we find the explicit form of the characteristics in the small-g range,

$$t-t_0=\int_0^{g(t)}\frac{dg}{a(g)A_g(g)}, \quad g\ll\min_t g^*(t),$$
$$p=A_g(g), \quad R(g,t)\approx A(g). \tag{24}$$

The Hamiltonian equations (23) and the initial conditions (24) define a set of characteristics,

$$g=g(t,t_0), \quad p=p(t,t_0), \quad s=s(t,t_0), \tag{25}$$

that can be parameterized by one parameter, the instant t_0. The set is periodic in t_0, with period T, because the characteristics with t_0 and t_0+T coincide with each other.

We emphasize that, in the present paper, we investigate the case where t_0 is finite, i.e., integral (24) converges. This case is of interest for many models of nucleation. Analysis can be generalized to the case where $t_0\to-\infty$. In this latter case the problem of nucleation becomes very similar to the problem of activation escape of a periodically driven Brownian particle.[26]

The activation energy $R(g_f,t_f)$ equals the action $s(t_f,t_0)$ in Eq. (23) along the characteristic Eq. (25) with t_0 given by the boundary condition at the end point (g_f,t_f),

$$R(g_f,t_f)=\frac{1}{4}\int_{t_0}^{t_f}\frac{1}{a(g(t))}[\dot{g}-K(g(t))]^2\,dt,$$
$$g(t_0)=0,\quad g(t_f)=g_f. \tag{26}$$

Generically, the function $t_0=t_0(g_f,t_f)$ is multivalued [cf. Ref. 22(a) where a related effect was observed for a periodically driven dynamical system]. This means that, for given g_f,t_f, there are several characteristics in Eq. (25) with different values of t_0 and with different momentum at the final point $p(t_f,t_0)$. In this case one has to choose the value of $t_0=\bar{t}_0$ that provides the *least* action $s(t_f,\bar{t}_0)$, and the corresponding path $g=g(t,\bar{t}_0)$ will be the ''true'' optimal path for reaching size g_f at $t=t_f$. The paths that do not correspond to the global minimum of action Eq. (26) are *extreme* paths of the integral over time in Eq. (26) considered as a functional of the paths $g(t)$. Different extreme paths give different values to the action $R(g_f,t_f)$ in Eq. (26), which then becomes a multivalued function of the end point (q_f,t_f) (see Sec. IV A). The least action $\bar{R}(q_f,t_f)=s(t_f,\bar{t}_0)$ corresponds to the lowest sheet of this function.

The prefactor $C(g,t)$ in Eq. (21) can be found next to the leading order approximation in D by substituting Eq. (21) into FPE (3). Using Eq. (23) and the fact that Eq. (21) should match the Gibbs distribution Eq. (5) at small g, one obtains, after a straightforward calculation,

$$C(g_f,t_f)=n_0\exp\left[-\int_{t_0}^{t_f}r(g(t,t_0),t)\right]dt,$$
$$r(g,t)=\frac{\partial}{\partial g}\left(K+a\frac{\partial R}{\partial g}\right),\quad g(t_f,t_0)=g_f \tag{27}$$

[cf. Refs. 18, 29(c); and 27; the integral in Eq. (27) is taken along the optimal path that arrives at end point (g_f,t_f)].

B. Activation energy of nucleation

The activation energy of nucleation is determined by the probability density of reaching critical size $g^*(t)$. Once the nucleus size has approached critical value, it has a probability $\sim 1/2$ to grow to a supercritical size as a result of a small fluctuation; large fluctuations are no longer needed. Respectively, the activation energy is given by $R(g^*(t),t)$. Intuitively, one may expect that the latter quantity is independent of time in the general case of nonadiabatic driving described by Eqs. (23). This is related to the slowing down of the motion of the system as its size approaches $g^*(t)$. This size corresponds to the unstable periodic state of the system in the neglect of fluctuations; the closer the system is to $g^*(t)$ the slower $g-g^*(t)$ changes in time, according to the deterministic equation (8). As we show below, slowing down also occurs for the optimal fluctuational trajectory for nucleation (this is a very general feature known in the escape problem and is not limited to Markov processes[17(a)]). Over a long time of motion near $g^*(t)$, small fluctuations will ''smear'' the distribution and make R time independent.

The latter arguments can be put on quantitative basis if one notices that the activation energy of nucleation is given by the *extremum* of $R(g^*(t),t)$. The condition for R to be extremal with respect to the instant t where the critical size is reached, $dR(g^*(t),t)/dt\equiv a^*p^2=0$, shows that the optimal path of interest has $p\to 0$ when it approaches $g^*(t)$. It follows from Eq. (23b) that the momentum may become equal to zero only asymptotically as $t\to\infty$, in agreement with the qualitative arguments discussed above. For such a trajectory, the activation energy for nucleation,

$$R(g^*(t),t)=R_n, \tag{28}$$

is indeed independent of t.

To analyze paths $g(t),p(t)$ near the critical nucleus, we linearize in $g-g^*(t)$ and p the coefficients in the equations-of-motion (23) and keep only the quadratic terms in $p,z=g-g^*(t)$ in the Hamiltonian Eqs. (22),

$$\tilde{H}(z,p,t)\equiv H(g^*(t)+z,p,t)\approx a^*(t)p^2+K_g^*(t)pz. \tag{29}$$

Solving the corresponding linear equations we obtain

$$p(t,t_0)=k(t_0), \tag{30a}$$
$$g(t,t_0)-g^*(t)=-\beta(t)p(t,t_0)+\delta(t_0)u^{-1}(t,t_0),$$
$$|g-g^*|\ll g^*,\quad |p|\ll|\delta\mu|, \tag{30b}$$

where t_0 is the parameter of the set of extreme paths introduced in Eq. (24), the function $u(t,t')$ is given by Eq. (16), and

$$\beta(t)=\frac{2}{1-u^2(T,0)}\int_t^{t+T}a^*(\tau)u^2(\tau,t)\,d\tau. \tag{31}$$

[We note that $\beta(t)$ is periodic, with period T.] Coefficients $k(t_0)$ and $\delta(t_0)$ in Eqs. (30) are ''global''; they cannot be found from local analysis near the unstable periodic orbit and require integrating Eqs. (23) in the region far away from this orbit, where Eqs. (23) may not be linearized.

In Eq. (30), the function $u(t,t_0)$ decays exponentially in the limit of large $t-t_0$, and so does the momentum $p(t,t_0)$. Therefore in the expression for $g(t)-g^*(t)$ the first term $\propto p(t,t_0)$ decays at large times, whereas the second term grows exponentially. This latter term corresponds to purely deterministic paths in Eq. (8) that diverge from the unstable periodic state $g=g^*(t)$. Due to the admixture of this term the characteristics, in general, will *miss* the unstable periodic orbit. However, the characteristic that satisfies the condition,

$$\delta(t_0^*)=0, \tag{32}$$

will not diverge; it will approach the periodic orbit asymptotically for $t\to\infty$. This characteristic corresponds to the most probable nucleation path (MPNP) $g(t,t_0^*)$ along which the system is most likely to evolve when the critical nucleus is formed.

The activation energy for nucleation R_n is determined by the action along the MPNP

$$f^*(t)\propto\exp[-R_n/D],$$
$$R_n=\frac{1}{4}\int_{t_0^*}^{\infty}\frac{1}{a(g(t))}[\dot{g}-K(g(t))]^2dt, \tag{33}$$
$$g(t_0^*)=0,\quad g(t\to\infty)\to g^*(t).$$

In general, Eq. (32) will have several roots per period of driving force T. The MPNP corresponds to root t_0^* which

provides the least value of action in Eq. (33). Note that there is a periodic set of MPNPs which repeat each other with the period of the force, $g(t,t_0^*)=g(t+nT,t_0^*+nT)$.

Equation (33) provides the basis of the *nonadiabatic* theory of nucleation rate in periodically driven systems. An important feature of this theory is the time independence of the nucleation rate, despite the fact that the MPNPs are synchronized with the driving force, as discussed above (cf. Refs. 10, 20, 21). One can expect, however, that the effect of the driving force on the nucleation rate substantially depends on the interrelation between the force period T and the characteristic relaxation time of the nuclei of a nearly critical size.

Indeed, for nucleus size g close to the critical value $g^*(t)$, the deviation $g-g^*(t)$ varies in time exponentially [cf. Eqs. (8), (30)], and generically a nucleus will leave the vicinity of $g^*(t)$ [where $|g-g^*(t)|\lesssim(\beta^*D)^{1/2}$] over a characteristic relaxation time $t_r\sim 1/K_g^*$. On the other hand, the nuclei are ''injected'' into this vicinity along the MPNPs $g(t,t_0^*+nT)$ with the time interval equal to period T of the driving force. If this period is small, $t_r\gtrsim T$, then the number of nuclei with $g\approx g(t)$ only slightly oscillates in time, and the value of $f^*(t)$ is determined to logarithmic accuracy by R_n in Eq. (33).

For smaller frequencies of the driving force, the nuclei that reached critical size along the MPNP will have left the vicinity of $g^*(t)$ before the next MPNP arrives. As a result, the amplitude of the oscillations of the population of the critical size $f^*(t)$ (and therefore the nucleation rate) will increase as the driving frequency decreases. Eventually there will be reached a completely adiabatic regime where the population of the critical size at an instant t is determined by the optimal path that has come closest to $g^*(t)$ within a time interval $\sim t_r\ll T$, i.e., for a given instantaneous value of the force. Respectively, the nucleation rate $\mathcal{J}_0(t)$ will follow the instantaneous value of the chemical potential $\delta\mu(t)$,

$$\mathcal{J}_0(t)\propto\exp\left[-\frac{\Phi_0(\tilde{g}^*(t))}{k_BT}\right],\quad \left[\frac{\partial\Phi_0}{\partial g}\right]_{g=\tilde{g}^*(t)}=0. \tag{34}$$

The time dependence of the distribution of supercritical nuclei also depends extremely strongly on the driving frequency. Supercritical growth does not require large fluctuations and therefore deep in the nonadiabatic regime $f(g,t)$ only weakly depends on time for $g-g^*(t)\gg(\beta^*D)^{1/2}$. In contrast, in the adiabatic regime where $f^*(t)$ is oscillating in time *exponentially* strongly, the distribution of supercritical nuclei does likewise.

IV. NUCLEATION RATE FOR MODERATELY STRONG ac MODULATION

In this section, the central section of the paper, we investigate the case in which the ac component of supersaturation $\delta\mu(t)$ is comparatively small, so that in Eq. (2)

$$|h(t)/\delta\mu_0|\ll 1. \tag{35}$$

In this case the ac driving-force-induced change $\Delta R(g,t)$ of the activation energy is much less than activation energy $\Phi_0(g)$ in the absence of force. However, the modulation amplitude can still be sufficiently strong to change the activation energy by an amount greater than D, that is,

$$R(g,t)=\Phi_0(g)+\Delta R(g,t),\qquad |\Delta R|\ll\Phi_0,\quad \exp[|\Delta R|/D]\gg 1. \tag{36}$$

Therefore the ac modulation makes an *exponentially* strong effect on the distribution function $f(g,t)$ and the nucleation rate $\mathcal{J}$.

In the absence of driving ($h(t)=0$), Eq. (23) for the optimal fluctuational paths has solutions which are just the time-reversed paths of the deterministic dynamics of nuclei in the neglect of fluctuations Eq. (8). Time-reversal symmetry between fluctuational and deterministic paths is a generic property of thermal equilibrium systems.[28] The unperturbed optimal path $g=g_0(t-t_0)$ depends on the initial instant of growth t_0 only through the elapsed time $t-t_0$,

$$t-t_0=-\int_0^{g_0(t-t_0)}\frac{dg}{K_0(g)},\quad K_0(g)=-a(g)\frac{d\Phi_0(g)}{dg}. \tag{37}$$

Note that this expression is similar to Eq. (24) for the optimal paths at small g where instead of free energy $\Phi_0(g)$ we used surface energy $A(g)$.

To the first order in $h(t)$, the driving-force-induced change of $R(g_f,t_f)$ is given by the terms $\propto h(t)$ in the integrand in Eq. (26) evaluated along the unperturbed optimal path,

$$\Delta R(g_f,t_f)=-\int_{t_0}^{t_f}h(t)\dot{g}_0(t-t_0)dt,\qquad g_0(0)=0,\quad g_0(t_f-t_0)=g_f. \tag{38}$$

As in the case of the activation energy for a large fluctuation, the driving-force-induced correction to the prefactor of the distribution $C(g,t)$ Eq. (27) is $\propto h$; however, in contrast to the exponent of the distribution, the correction to the prefactor is not divided by the small noise intensity D. Therefore, for comparatively weak driving force Eq. (35), the prefactor $C(g,t)$ changes only slightly. Function $r(g,t)$ in Eq. (27) vanishes for the unperturbed optimal path Eq. (37), and thus $C=n_0$ for $h\to 0$. Therefore, for arbitrary h/D but for small $h/\delta\mu_0$ the steady-state distribution of subcritical nuclei takes the form

$$f(g,t)=n_0\exp[-R(g,t)/k_BT], \tag{39}$$

where $R(g,t)$ is determined in Eqs. (36) and (38).

A. Nonadiabatic theory of nucleation rate: The activation energy

In the absence of driving, the activation energy of nucleation Φ_0^* as calculated along the optimal paths $g_0(t-t_0)$ is independent of the instant t_0 when nuclei start to grow. The driving force lifts this time degeneracy. As discussed in Sec. III B, in general there will be only one most probable nucleation path (MPNP) per force period, with appropriate $t_0=t_0^*$. This path will asymptotically approach the critical nucleus, whereas other paths (with $t_0\neq t_0^*$) will miss it. Because of that, the direct perturbation expansion of the characteristics Eq. (25) in powers of the driving force will also diverge near the unstable periodic state. Physically, this is a

consequence of the slowing down of motion near the periodic state, which gives rise to accumulation of the effect of perturbation. Formally, this can be seen from Eqs. (30) and (31).

Function $u(t,t_0)$ in Eq. (30) grows exponentially in time, and so does the second term in the expression for $g(t,t_0)$, which is $\propto \delta(t_0)$. The first term in this expression is $\propto p(t,t_0)$ and decays in time exponentially. Therefore it is the second term which describes the deviation of the path from the MPNP. This term is due to the ac driving force; it is equal to zero for $h(t)=0$, because the unperturbed optimal paths Eq. (37) approach critical size g_0^* for all values of t_0. The perturbation expansion of path $g(t,t_0)$ in $h(t)$ becomes inapplicable for sufficiently large t where both terms in Eq. (30b) are of the same order of magnitude.

Based on the results of Refs. 10 and 20 expressions (30) for the characteristics in the vicinity of the unstable periodic state can be written in explicit form. We note first that, to the first order in the driving force amplitude, the unstable state is given by the expression

$$g^*(t)=g_0^*+a^*\sum_{n\neq 0}\frac{h_n}{i\omega n-\lambda^*}\exp(i\omega n t). \tag{40}$$

To zeroth order in h, the function $u(t,t')$ in Eq. (30) is equal to $\exp[-\lambda^*(t-t')]$, whereas the function $\beta(t)$ Eq. (31) is equal to β^*, where

$$\frac{1}{\beta^*}=-\Phi_0''(g_0^*),\quad \lambda^*=-a(g_0^*)\Phi_0''(g_0^*), \tag{41}$$

with g_0^* being the critical nucleus size in the absence of the ac driving force, $\Phi_0'(g_0^*)=0$.

The idea of the calculation is to solve the equations for the characteristics Eqs. (23) and (24) perturbatively in $h(t)$ in the region far from the critical nucleus. On the other hand, we already know the solution Eq. (30) for the characteristics in the region where deviation g^*-g is much less than g^*. This solution applies for all driving forces. We can now match these two solutions in the range of small, but not too small, g_f-g, where they both apply. Finally, we obtain to the leading order in the driving force amplitude

$$p(t,t_0)=k^*\exp[-\lambda^*(t-t_0)], \tag{42a}$$

$$g(t,t_0)-g^*(t)=-\beta^* p(t,t_0)+\delta(t_0)\exp[\lambda^*(t-t_0)], \tag{42b}$$

$$s(t,t_0)=\Phi_0^*-\frac{\beta^*}{2}p^2(t,t_0)+U(t_0), \tag{42c}$$

where

$$U(t_0)=\sum_{n\neq 0}h_n\chi(n\omega)\exp(in\omega t_0),$$

$$\delta(t_0)=\frac{1}{\lambda^* k^*}\dot{U}(t_0), \tag{43}$$

and

$$k^*=\frac{g_0^*}{\beta^*}\exp[\lambda^*\tau^*],$$

$$\tau^*=\int_0^{g_0^*}dg\left[\frac{1}{a(g)d\Phi_0(g)/dg}-\frac{1}{\lambda^*(g_0^*-g)}\right]. \tag{44}$$

Function $\chi=\chi(\omega)$ in the expression for $U(t)$ is the logarithmic susceptibility for nucleation.[10,20] It describes the frequency-dependent change of the activation energy of nucleation, which is linear in the driving force amplitude, as discussed in Sec. V,

$$\chi(\omega)=-\int_0^\infty dt\dot{g}_0(t)\exp[i\omega t]dt, \tag{45}$$

where $g_0(t)$ is the unperturbed optimal nucleation path defined in Eq. (37).

It is seen from Eqs. (42) and (43) that sufficiently close to the critical state, $|g-g^*|\sim|h|^{1/2}$, the first and second terms in the expression for $g(t,t_0)$ in Eq. (42b) are of the same order of magnitude, which explicitly shows where the perturbation theory in h does not apply.

Function $R(g,t)$ can now be found from $s(t,t_0)$ and $g(t,t_0)$ using Eqs. (23c), (42), and (43). In the region $|g-g^*|\gg|h|^{1/2}$ the first term in Eq. (42b) largely exceeds the second term, and $R(g,t)$ is given by the perturbation theory Eq. (38). However, in the region $|g-g^*|\sim|h|^{1/2}$ the equation $g=g(t,t_0)$ has more than one root t_0 for given g,t. This gives rise to *multivaluedness* of the function $R(g,t)$ as pointed in Sec. III A. The form of action $R(g,t)$ in this region can be conveniently studied by making a transformation to new canonical variables, where the coordinate corresponds to the ''old'' momentum p. The relation between $R(g,t)$ and action $W(p,t)$ in the new variables is

$$\begin{aligned} &R(g,t)=p[g-g^*(t)]+W(p,t),\\ &g-g^*(t)=-\frac{\partial W(p,t)}{\partial p},\quad p=\frac{\partial R(g,t)}{\partial g}, \end{aligned} \tag{46}$$

where $p(g-g^*(t))$ is the generating function of the transformation.[25]

In the new variables, action $W(p(t,t_0),t)\equiv w(t,t_0)$ on the characteristics Eq. (42) can be found directly, because $R(g(t,t_0),t)\equiv s(t,t_0)$ is known from Eq. (42c). Moreover, the equation $p=p(t,t_0)$ has a single root t_0 for given p,t, and therefore

$$W(p,t)=\Phi_0^*+\frac{\beta^*}{2}p^2+U\left(t+\frac{1}{\lambda^*}\ln\left(\frac{p}{k^*}\right)\right). \tag{47}$$

The dependence of the action $W(p,t)$ on p for a given t is shown in Fig. 1. The function $W(p,t)$ is single valued; in the limit of small p it oscillates with a nearly constant amplitude and with the frequency which diverges logarithmically as $p\to 0$. In order to determine $R(g,t)$ one has to express p in terms of g from the equation $g-g^*(t)=-\partial W(p,t)/\partial p$, and then put it into Eq. (46). Because function $U(t_0)$ is periodic, with the period $2\pi/\omega$, it is clear that there will be infinitely many roots, p_n, which scale approximately as $p_n\propto\exp[-2\pi n\lambda/\omega]$ for large n. Each p_n corresponds to the extreme path $g=g(t,t_0^n)$, with the initial in-

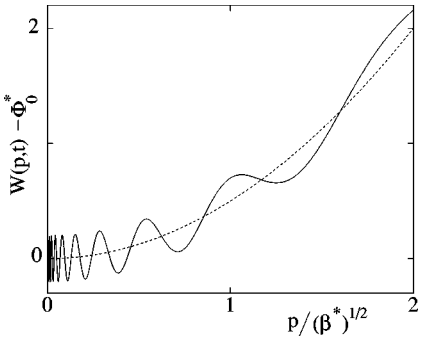

FIG. 1. Solid curve: action function $W(p,t)$ vs momentum p in the presence of the driving, for a given time t (units are arbitrary). Dashed curve: action function $W(p,t)$ for zero driving.

stant t_0^n which is equal to the argument of U in Eq. (47) for a given p_n. All of these paths come through the same point g at the instant t, but with different momenta p_n, and they also provide different values to the action $R(g,t)$. As we discussed in Sec. III A, one needs to select the root $\overline{p_n}$ which provides the global minimum to $R(g,t)$.

We will not investigate here the detailed structure of the surface of the minimum action $\overline{R}(g,t)$ (see Refs. 23, 21). Instead, we will be interested in the value of $\overline{R}(g,t)$ directly at the periodic unstable state, $g=g^*(t)$. This value of $\overline{R}$ gives the nucleation rate, to logarithmic accuracy, cf. Eq. (28). From condition $g=g^*(t)$ and Eq. (46), it follows that p is given by the condition

$$\partial W(p,t)/\partial p=0. \tag{48}$$

We need to find the root of this equation that provides the global minimum to $W(p,t)$ and, from Eq. (46), the minimal value of $W(p,t)$ is equal to $\tilde{R}(g^*(t),t)$. It immediately follows from the form of $W(p,t)$ in Eq. (47) (see also Fig. 1) that the global minimum of $W(p,t)$ is achieved in the asymptotic limit of $p\to 0$ where the second term $\propto p^2$ can be neglected. Then $W(p,t)$ becomes minimal where U is minimal, that is for

$$\dot{U}(t_0^*)=0, \tag{49}$$

which precisely corresponds to the condition for the MPNP $g(t,t_0^*)$ as given by Eqs. (42b), (43), and (32).

The corresponding activation energy for nucleation is (cf. Refs. 10, 20)

$$R_n=\Phi_0^*+U^*, \quad U^*\equiv\min_{t_0} U(t_0)=U(t_0^*). \tag{50}$$

The quantity U^* gives the driving-force-induced correction to the nucleation barrier. It immediately follows from Eq. (38) that this quantity is just equal to $\lim_{t\to\infty}\Delta R(g_0(t,t_0^*),t)$ evaluated along the unperturbed optimal path with the appropriate initial instant t_0^*.

By construction, function $U(t_0)$ in Eq. (43) is periodic, with force period T and zero mean. Therefore its minimal value is negative, $U^*<0$, which means that ac modulation always exponentially *increases* nucleation rate.[10,20]

Monochromatic driving

For sinusoidal modulation of the chemical potential,

$$\delta\mu(t)=\delta\mu_0+2\,\delta\mu_1\cos\omega t, \tag{51}$$

the function $U(t_0)$ takes a simple form,

$$U(t_0)=2\,\delta\mu_1|\chi(\omega)|\cos[\omega t_0+\arg\chi(\omega)], \tag{52}$$

and the initial instant t_0^* at which the MPNP starts is equal to

$$t_0^*=\frac{1}{\omega}[\pi(2n+1)-\arg\chi(\omega)]. \tag{53}$$

The driving-force-induced change of the logarithm of distribution $f(g,t)$ for the critical nucleus size $g^*(t)$,

$$\ln f^*(t)\approx-\frac{\Phi_0^*}{D}+2\,\frac{\delta\mu_1|\chi(\omega)|}{D}, \tag{54}$$

is linear in the driving force, which explains why we call $\chi(\omega)$ the logarithmic susceptibility (LS).[10,20]

B. Nonadiabatic theory of nucleation rate: The prefactor

The prefactor Analysis of the prefactor in the nucleation rate requires calculation of the probability flux $j(g,t)$ Eq. (4) with account taken of the periodic driving. To do this we will analyze the distribution function in the vicinity of critical state $g^*(t)$ using the results of the previous section and Eq. (13) for the function $\tilde{f}(z,t)\equiv f(g^*(t)+z,t)$. Equation (13) is linear in z, and this allows us to seek its solution using the Laplace transformation,

$$\tilde{f}(z,t)=\int_0^{+\infty}d\rho\,\exp\left[-\frac{1}{D}(\rho z+V(\rho,t))\right]. \tag{55}$$

We assume that $\exp[-V(\rho,t)/D]$ does not diverge for $\rho\to 0$ and decays sufficiently fast for $\rho\to\infty$ (these assumptions will be verified later). From Eqs. (13) and (55) we obtain the following equation for the function $V(\rho,t)$:

$$\frac{\partial V}{\partial t}-K_g^*(t)\rho\,\frac{\partial V}{\partial\rho}+a^*(t)\rho^2=Da_g^*(t)\rho. \tag{56}$$

We are looking for a time-periodic solution of Eq. (56), $V(\rho,t)=V(\rho,t+2\pi/\omega)$. The boundary conditions for $V(\rho,t)$ can be found by matching distribution $\tilde{f}(z,t)$ to the asymptotic expression Eq. (21). The matching should be done in the region where, on the one hand, $|z|$ is sufficiently large so that the integrand in Eq. (55) is a steep function of ρ and the integral over ρ can be evaluated by the steepest descent method, but on the other hand, $|z|\ll g^*(t)$, so that Eq. (13) is still applicable.

If the integral over ρ Eq. (55) can be evaluated by the steepest descent, then

$$\tilde{f}(z,t)=\tilde{C}\exp\left[-\frac{1}{D}(z\rho_m+V(\rho_m,t))\right],$$

$$\tilde{C}=\left(\frac{2\pi D}{|\partial^2V/\partial\rho^2|}\right)^{1/2}, \tag{57}$$

$$z=-\frac{\partial V(\rho,t)}{\partial\rho}\quad\text{for}\quad\rho=\rho_m\quad(|z|\ll g^*).$$

Here $\rho_m=\rho_m(z,t)$ is the position of the global maximum of the integrand in Eq. (55) for given z and t, and the prefactor $\tilde{C}$ is evaluated at $\rho=\rho_m$.

Function $\tilde{f}(z,t)$ in Eq. (57) has exactly the same form as that given by Eqs. (39) and (46). In particular, it is immediately seen that the relation between functions $R(g,t)\equiv\tilde{R}(z,t)$ and $V(\rho,t)$ in the exponents of the expressions for $\tilde{f}$ corresponds to the canonical transformation Eq. (46) to the basis where ρ equals to the momentum p. This means that $V(\rho,t)=W(\rho,t)$, with an accuracy to the terms $\sim D$.

It follows from the canonical transformation Eq. (46) that function $W(p,t)$ obeys the Hamilton–Jacobi equation

$$\frac{\partial W}{\partial t}+\tilde{H}\left(-\frac{\partial W}{\partial p},p,t\right)=0, \tag{58}$$

where the Hamiltonian near critical state $\tilde{H}(g-g^*(t),p,t)$ is given by Eq. (29). Clearly, the equations for $W(p,t)$ and $V(p,t)$ coincide in the neglect of the small term $Da_g^*\rho\ll D$ in Eq. (56). This means that, in fact, we know the solution of Eq. (56), as functions $V(p,t)$ and $W(p,t)$ can differ only by a constant and, from the matching condition, this constant should go to zero as $D\to 0$, so that we can write

$$V(p,t)=W(p,t)-D\ln c_0. \tag{59}$$

Constant c_0 can be determined by matching the prefactors in Eqs. (57) and (39). With account taken of the explicit form of $W(p,t)$, this gives

$$c_0=n_0\left(\frac{\beta^*}{2\pi D}\right)^{1/2}. \tag{60}$$

The above expression, combined with Eqs. (55), (59), and (47), explicitly determines the steady-state distribution near the critical nucleus. After changing to $\xi=(D/\beta^*)^{-1/2}\rho$ in Eq. (55), we finally obtain

$$\tilde{f}(z,t)=f_0^*\left(\frac{2}{\pi}\right)^{1/2}\int_0^\infty d\xi\exp\left(-\frac{z\xi}{z_D}-\frac{1}{2}\xi^2\right)\times\exp\left[-\frac{1}{D}U\left(t-\tau_D+\frac{1}{\lambda^*}\ln\xi\right)\right], \tag{61}$$

$$f_0^*=\frac{n_0}{2}\exp\left[-\frac{1}{D}\Phi_0^*\right].$$

Here, f_0^* is the concentration of the critical nuclei in the absence of driving, whereas

$$z_D=(D\beta^*)^{1/2},\quad \tau_D=\tau^*+\frac{1}{\lambda^*}\ln\left(\frac{g_0^*}{z_D}\right). \tag{62}$$

The parameter z_D defines the characteristic region near the critical nucleus where the motion is dominated by small fluctuations. Time τ_D gives the characteristic time $t-t_0$ it takes for the nucleating system to reach region $g^*(t)-g\sim z_D$ moving along the optimal path. This time is the sum of the ''fast'' time τ^* defined in Eq. (44), which corresponds to the motion far from the critical state, $g_0^*-g\gg z_D$, and the characteristic duration of motion near the critical state.

Expression (61) is one of the central results of the paper. It gives the nuclei distribution function in the critical region in the presence of ac modulation of the chemical potential. In the case of not very strong driving, the effect of modulation manifests itself entirely through the factor $\exp[-U/D]$ in the integrand, where $U=U(t_0)$ is defined in Eq. (43) and is proportional to the driving amplitude. In the limit of very weak driving, $|U/D|\ll 1$, the distribution $\tilde{f}(z,t)$ in Eq. (61) goes over into the stationary distribution $\tilde{f}_0(z)$ near the critical nucleus known from the classical droplet theory of nucleation (cf. Refs. 1–3).

Time-averaged nucleation rate

A sufficiently strong driving, for which $|U|/D\gg 1$ in Eq. (61), results in the exponentially strong change of the nucleation rate. Using Eq. (61) one can obtain the distribution function averaged over the force period, and also the average value of flux $\tilde{j}(g,t)$. Averaging of the integrand in Eq. (61) over t gives a factor

$$A=\langle e^{-U(t)/D}\rangle, \tag{63}$$

which can be taken outside the integral. For sufficiently strong driving it can be evaluated by the steepest descent method. The dominant contribution to Eq. (63) is given by the value of t which corresponds to the MPNP. The result has the form

$$\langle\tilde{f}(g,t)\rangle=A\tilde{f}_0(z),\qquad A\approx\left(\frac{2\pi D}{T^2\ddot{U}(t_0^*)}\right)^{1/2}\exp\left(-\frac{U^*}{D}\right)\gg 1, \tag{64}$$

where $\tilde{f}_0(z)$ is the stationary distribution function for $h(t)=0$ [it can be obtained by setting $U=0$ in Eq. (61)]. Distribution Eq. (64) differs from this stationary distribution by an exponentially large factor; so does the average nucleation rate, $\tilde{\mathcal{J}}/\mathcal{J}_0=A$.

In the case of monochromatic driving, $h(t)=2h_1\times\cos(\omega t)$, from Eqs. (52) and (63) we obtain for the average nucleation rate

$$\frac{\tilde{\mathcal{J}}}{\mathcal{J}_0}=A=I_0\left(\frac{1}{\epsilon_1}\right),\quad \epsilon_1\equiv\frac{D}{2h_1|\chi(\omega)|}, \tag{65a}$$

$$A\approx\left(\frac{\epsilon_1}{2\pi}\right)^{1/2}\exp\left(\frac{1}{\epsilon_1}\right),\quad \epsilon_1\ll 1, \tag{65b}$$

$$A\approx 1+\frac{1}{4\epsilon_1^2}=1+\left(\frac{h_1|\chi(\omega)|}{D}\right)^2,\quad \epsilon_1\gg 1, \tag{65c}$$

where $I_0(x)$ is the modified Bessel function.[29]

Equation (65a) determines the average nucleation rate for an *arbitrarily strong* driving and in the *general* case of nonlinear growth law Eq. (37). The average rate depends on a single dimensionless parameter ϵ_1, in which the only model-dependent factor is the absolute value of the logarithmic susceptibility $\chi(\omega)$ Eq. (45).

C. Distribution function for nuclei of the critical size

In this subsection we consider the distribution $\tilde{f}(z,t)\equiv f(g^*(t)+z,t)$ in the region dominated by small fluctua-

tions. For simplicity, we will set $z=0$ in Eq. (61) and analyze explicitly the distribution function $f^*(t)$ evaluated exactly at the size of the critical nucleus. We will be interested in the nontrivial case of comparatively strong driving where the factor $\propto \exp[-U/D]$ in the integrand in Eq. (61) varies with ξ exponentially steeply and the integral can be evaluated by the steepest descent method.

Remember that the dimensionless variable ξ in Eq. (61) corresponds to the momentum p of the auxiliary system Eq. (22) near the critical state. The values of ξ can also be parameterized by the instant t_0 at which begins the characteristic with $p(t,t_0)=(D/\beta^*)^{1/2}\xi$. From Eq. (42)

$$\xi=\exp[-\lambda^*(t-\tau_D-t_0)]. \tag{66}$$

This parameterization allows us to think of the distribution $f^*(t)$ Eq. (61) as a sum of the contributions from various extreme paths that start at different t_0 and approach the critical region $\xi\sim 1$ (and $|z|=|g-g^*(t)|\sim z_D$) within *finite* time. Changing to integration over t_0 in Eq. (61), we obtain that, for the critical nucleus ($z=0$),

$$f^*(t)=f_0^*\left(\frac{\pi}{2}\right)^{1/2}\lambda^*\int_{-\infty}^{\infty}dt_0 G^*(e^{-\lambda^*(t-\tau_D-t_0)}) \times\exp\left[-\frac{1}{D}U(t_0)\right], \tag{67}$$

$$G^*(y)=y\exp\left[-\frac{1}{2}y^2\right].$$

It follows from this expression that the relative probabilities for the paths to reach critical state $z=0$ are mostly determined by the steep exponential factor $\exp[-U(t_0)/D]$. The ''window'' function $G^*(\xi)$ is comparatively smooth (for $\xi\sim 1$, it varies by a factor of ~ 1 when t_0 varies by the period T, provided $\lambda T\lesssim 1$). This function determines the time dependence of $f^*(t)$. In this approximation, the major contribution to the integral Eq. (67) comes from the values

$$t_0^n=t_0^*+nT,\quad n=0,\pm 1,\pm 2,...,\quad T=\frac{2\pi}{\omega}, \tag{68}$$

for which the factor $\exp[-U(t_0^*)/D]$ is maximal. This precisely corresponds to the result given by Eqs. (49) and (50) for the activation energy of nucleation, with t_0^*+nT being just the initial instants at which the MPNPs start (generically, there is one MPNP per period T).

The corresponding stationary points $\xi=\xi_n(t)$ of the integral in Eq. (61) for $z=0$ are

$$\xi_n(t)=\exp[-\lambda^*(t-\tau_D-t_0^n)]. \tag{69}$$

Finally, for the function $f^*(t)$ in Eq. (67) we obtain

$$f^*(t)=f_0^*A\Lambda^*(t),$$

$$\Lambda^*(t)=\lambda^*T\sum_{n=-\infty}^{\infty}G^*(\xi_n(t)), \tag{70}$$

where A is given in Eq. (64).

It follows from Eq. (70) that, for nonadiabatic driving, the distribution function $f^*(t)$ at the size of the critical nucleus $g^*(t)$ is given by the sum of the contributions from different MPNPs and from the paths within the tubes of fluctuational paths surrounding the MPNPs. Far from the critical size, the distribution of the paths within the tubes is nearly Gaussian, with variance $\sim D$. The contribution from the nth MPNP is determined by the portion of paths which reach $g^*(t)$ for a given position of the MPNP $g(t,t_0^n)$. It is described by the function $G^*(\xi_n)$. Clearly, it falls down exponentially for the MPNPs, which are still far away from $g^*(t)$, for given t. We note that the time dependence of $f^*(t)$ is fully determined by the factor $\Lambda^*(t)$. The latter factor does not depend on the spectrum of the driving force.

Low-frequency driving

In the limit of relatively low frequency of the driving force,

$$\exp[-\lambda^*T]\ll 1, \tag{71}$$

the function $\Lambda^*(t)$ has a form of periodic spikes, with width $\ll T$. In this case the terms with different n in expression (70) for $\Lambda(t)$ differ exponentially strongly, and at a given instant of time t there will be, in general, only one term in the sum over n, with n equal to a certain integer p, which will be dominating,

$$\Lambda^*(t)\approx\lambda^*TG^*(e^{-\lambda^*(t-\tau_D-t_0^p)}). \tag{72}$$

This term corresponds to the MPNP that has arrived at the critical region $\xi_n\sim 1$ at the instant $t_0^p+\tau_D$. Since function $G^*(\xi)$ is maximal for $\xi=1$, the maximum of $\Lambda(t)$ is reached at the instant $t=t_{\max}^p$, where,

$$t_{\max}^p=t_0^p+\tau_D,\quad \Lambda^*(t_{\max}^p)=\lambda^*T\exp(-1/2). \tag{73}$$

For $t-t_{\max}^p>1/\lambda^*$, the occupation of the unstable critical state decreases exponentially in time because the system moves away from this state. This decay is described by the factor $\exp[-2\lambda^*(t-t_{\max}^p)]$. At sufficiently large $t-t_{\max}^p$ the contribution from the next MPNP (the one that starts one period later) becomes important, and eventually $\Lambda^*(t)$ is described by Eq. (72) with p replaced by $p+1$.

The time dependence of $\Lambda^*(t)$ is strongly asymmetric with respect to $t-t_{\max}^p$. For $t<t_{\max}^p$ the occupation of the critical state is determined not by the relaxation away from it, but by the width of the tube of fluctuational paths surrounding the MPNP. This corresponds to the Gaussian decay of function $G^*(\xi)$ at large $\xi\gg 1$. Therefore for $t<t_{\max}^p$ the occupation of the critical state decreases much faster then for $t>t_{\max}^p$. The minima $t_{\min}^p$ of function $\Lambda^*(t)$ are close to its maxima, $t_{\max}^p-t_{\min}^p\ll T$. The values of $t_{\min}^p$ can be obtained by taking into account the contribution not only from the pth MPNP, but also from the MPNP that started a period earlier, i.e., at $t=t_0^{p-1}$. This gives

$$t_{\min}^p=t_0^p+\tau_D-\frac{1}{2\lambda^*}\ln(2\lambda^*T),$$

$$\Lambda^*(t_{\min}^p)=(2\lambda^*T)^{3/2}\exp[-\lambda^*T]. \tag{74}$$

For $t<t_{\min}^p$ the occupation of the critical state is determined by the MPNP with $n=p-1$ in Eq. (73).

D. Nucleation rate and probability distribution for supercritical nuclei

We now consider the distribution of supercritical nuclei far away from the small-fluctuation region, i.e., for $g-g^* \gg z_D$, but for $g-g^* \ll g^*$. The nucleation rate $\mathcal{J}(z,l)$ can be obtained by substituting the distribution function Eq. (61) into Eq. (14). Changing in Eq. (61) from ξ to t_0, we obtain

$$\frac{\mathcal{J}(z,t)}{\mathcal{J}_0}=\lambda^*\int_{-\infty}^{\infty}dt_0 G\left(\frac{z}{z_D}e^{-\lambda(t-\tau_D-t_0)}\right)\times\exp\left[-\frac{U(t_0)}{D}\right],\quad G(y)=y\exp[-y] \tag{75}$$

[we have neglected the term $-\xi^2/2$ in the exponent of the integrand in Eq. (61), which is $\propto(z_D/z)\ll 1$].

For the moderately strong driving in which we are interested, the probability flux is nearly constant along the deterministic growth paths, which are given by Eq. (8) with $h(t)$ set equal to zero. Therefore flux $j(g,t)$ equals $\mathcal{J}(z,t')$ where points (g,t) and (z,t') are connected by the deterministic path Eq. (8). The expression for flux $j(g,t)$ can then be written as

$$\frac{j(g,t)}{\mathcal{J}_0}=\lambda^*\int_{-\infty}^{\infty}dt_0 G(e^{-\lambda^*(t-\tau_0(g)-\tau_D-t_0)})\times\exp\left[-\frac{U(t_0)}{D}\right],\quad \tau_0(g)=\int_{g_0^*+z_D}^{g}\frac{dg}{K_0(g)}. \tag{76}$$

We have set $z=z_D$ in Eq. (75) and neglected in $j(g,t)$ the small terms $\propto\dot{g}^*(t)$. The function $\tau_0(g)$ in Eq. (76) is the time it takes for a nucleus to grow from size $g_0^*+z_D$ to size g.

Equation (76) is one of the central results of the paper. It provides the expression for the nucleation rate in a periodically driven system in a broad range of driving force strengths. Similar to Eq. (65a), it applies for weak forces, $|U(t)/D|\ll 1$, as well as for relatively strong forces $|U(t)/D|\gg 1$. Oscillations of the current for different values of g have the same form but differ from each other by a time-independent phase factor. The form of these oscillations is given in terms of the increment λ^* in the critical region, and also LS $\chi(\omega)$ which depends on a particular nonlinear model $K_0(g)$ and determines the form of function $U(t)$ for a given driving force $h(t)$.

For $|U(t)/D|\gg 1$, the integral over t_0 in Eq. (76) can be evaluated by the steepest descent method,

$$j(g,t)=\mathcal{J}_0\lambda^* TA\sum_{n=-\infty}^{\infty}G(e^{-\lambda^*[t-\tau_0(g)-t_0^n]}). \tag{77}$$

The values of t_0^n and A are given in Eqs. (68) and (64), respectively.

In the limit Eq. (71) of relatively low driving frequency, the sum in Eq. (77) is, in general, determined by the term with $n=p$,

$$j(g,t)=\mathcal{J}_0\lambda^* TAG(e^{-\lambda^*(t-\tau_0(g)-t_{\max}^p)}), \tag{78}$$

where $t_{\max}^p$ is given by Eq. (73). The current is maximal for the deterministic paths that arrive at state g for $t=t_{\max}^p+\tau_0(g)(p=0,\pm 1...)$ and start near the critical state at $t=t_{\max}^p$, at which the corresponding MPNPs arrives to this state and the probability density $f^*(t)$ is maximal [Eq. (73)].

Thus the value of the nucleation rate varies periodically, taking the maximal value

$$j_{\max}=j(t_{\max}^p+\tau_0(g),g)=\mathcal{J}_0 A\lambda^* T\exp(-1). \tag{79}$$

Similar to the analysis in the previous subsection, the minimal value of current $j(g,t)$ is reached where there occurs switching from one MPNP to another and one should keep two terms in the sum Eq. (77),

$$j_{\min}=j\left(g,t_{\max}^p+\tau_0(g)-\frac{1}{\lambda^*}\ln\lambda^* T\right)=2j_{\max}\lambda^* T\exp[-\lambda^* T]. \tag{80}$$

We note that the oscillations of current $j(g,t)$ in the supercritical range, as described by Eq. (77), differ from the oscillations of the distribution function $f^*(t)$ at the critical state, although they are closely related to each other. The difference comes from the fact that function $G^*(y)$ in Eq. (70) describes the diffusion near the critical state whereas, function $G(y)$ in Eq. (77) is defined in the supercritical region where growth dominates over diffusion processes. However, the supercritical current is also very asymmetric in time near its maxima, because the growth trajectories emanate from the critical state, and the current is larger for the trajectories that lag the MPNP as compared to the trajectories that lead the MPNP.

E. Nonadiabatic versus adiabatic driving

Expressions (70) and (77) correspond to the case of nonadiabatic driving. The essential feature of this case is that the exponential factor $\exp[-U(t_0)/D]$ in the integrands in expressions (67) and (76) is a much steeper function of t_0 than functions G^* and G, respectively. The latter functions vary only slightly within the characteristic widths of the maxima of $\exp[-U(t_0)/D]$ in the vicinity of the stationary points in the integral Eqs. (67) and (76). This is true provided

$$\lambda^*\left|\frac{D}{\ddot{U}(t_0^*)}\right|^{1/2}\ll 1. \tag{81}$$

In particular, for sinusoidal driving we obtain

$$\nu\equiv\frac{\omega}{\lambda^*}\gg\epsilon_1^{1/2}, \tag{82}$$

where $\epsilon_1=D/2h_1|\chi(\omega)|$ in Eq. (65a).

If the period of driving is very large, functions G^* and G in Eqs. (67) and (76) depend on t_0 steeper than $\exp[-U(t_0)/D]$, and for all t the major contribution to the integrals in Eqs. (67) and (76) comes from the vicinities of the values of t_0 where G^* and G are maximal. In the interesting case where $\max U(t)/D\gg 1$, this happens if

$$\max U(t)/\lambda^* TD\ll\lambda^* T\gg 1 \tag{83}$$

(i.e., $h_1|\chi(\omega)/D\ll\lambda^* T$, for monochromatic driving).

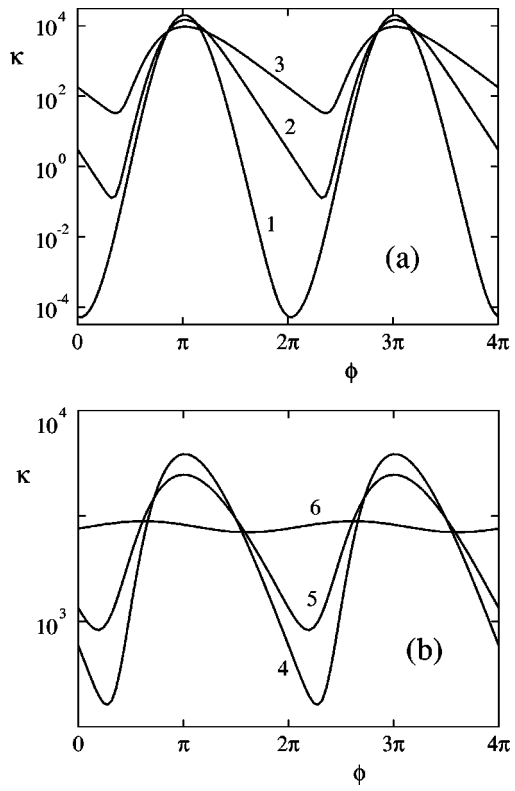

FIG. 2. Reduced nucleation rate $\kappa=\mathcal{J}/\mathcal{J}_0$ as a function of phase ϕ [Eq. (85)] for different values of the reduced driving frequency $\nu=\omega/\lambda^*$ and for the reduced driving force amplitude $2h_1|\chi(\omega)|/D=1/\epsilon_1=10$. Curves 1–6 correspond to $\nu=0.1$, 0.3, 0.6, 1, 1.3, 3.14.

For the slowly varying driving force Eq. (83), the characteristic duration of motion along the MPNP to the small-fluctuation region near the critical nucleus size is $\tau_D\sim 1/\lambda^* \ll 1/T$, and the time it takes a supercritical nucleus to reach size g is $\tau_0(g)\ll T$ for g not too different from g^*. Then expressions for the probability flux in the supercritical range and the population of the critical state are reduced to a purely adiabatic form

$$f^*(t)=f_0^*\exp\left[\frac{g_0^*h(t)}{D}\right],\quad j(g,t)=\mathcal{J}_0\exp\left[\frac{g_0^*h(t)}{D}\right]. \tag{84}$$

Here, $g_0^*h(t)=-\chi(0)h(t)$ is the adiabatic time modulation of the free energy $\Phi_0(g^*(t))$, to the leading order in the driving force amplitude.

We are now in a position to discuss the numerical results. For monochromatic driving, the time dependence of probability flux $j(g,t)$ in Eq. (76) is shown in Fig. 2. The flux is a periodic function of phase ϕ,

$$\phi=\omega(t-\tau_0(g)-\tau_D)+\arg\chi(\omega),$$

$$j(g,t)\equiv\mathcal{J}_0\kappa(\phi)=\sum_n j_n\exp[in\phi]. \tag{85}$$

Function $\kappa(\phi)$ is independent of g [cf. Eq. (76)], and depends only on the dimensionless reciprocal driving force amplitude ϵ_1 and the dimensionless force frequency ν.

Curves 1–6 in Fig. 2 correspond to the same ϵ_1 and different ν. Curve 1 corresponds to a very small ν and describes symmetric oscillations of the exponent of j in the purely adiabatic regime [cf. Eq. (84)]. Deviations from this behavior become more and more pronounced as ν increases. We note that the asymmetry of curves 2–4 is immediately related to the form of function $G(y)=y\exp[-y]$ in Eq. (76), with $y\propto\exp[-\lambda^*(t-t_0)]$. To the left from its maximum, function G displays a very steep (double-exponential) dependence on t. Therefore the dependence of flux j on ϕ to the left of the maxima is similar to the adiabatic behavior for small ν. The deviation from the adiabatic regime initially occurs in the regions to the right of the maxima. Indeed, as we discussed above, the maxima of j correspond to the periodic arrivals of MPNPs at the critical state, followed by slow diffusion near this state. This effect was noticed in Ref. 13 in the calculation of the probability flux over a periodically modulated parabolic barrier. It is clear from our analysis [cf. Eq. (80) and the discussion above it] that, for not too large ν, the minima of j as a function of phase ϕ are located to the left of the maxima and very close to them, as compared to 2π.

It is seen from Fig. 2 that, with increasing reduced frequency ν, oscillations in the nucleation rate are suppressed. In particular, curve 6 (where $\nu=\pi$) describes small-amplitude nearly sinusoidal oscillations of the flux about its average value in Eq. (65). Such *rectification* of the flux is due to the fact that, as the driving frequency increases the system, that has arrived to the ''slow'' area of small $|g-g^*|$ along one MPNP, it does not have time to leave this area before the next MPNP approaches it. Respectively, more and more MPNPs are contributing to the sum in Eq. (77). Generally, the amplitudes of nonzero Fourier harmonics j_n of the flux decrease exponentially with ω, for large ω/λ^*. In particular, for monochromatic driving,

$$\left|\frac{j_n}{j_0}\right|=\left(\frac{\pi n\nu}{\sinh(\pi n\nu)}\right)^{1/2},\quad \nu=\frac{\omega}{\lambda^*}. \tag{86}$$

Therefore in the limit $\exp[\pi\nu]\gg 1$ the nucleation rate is essentially rectified.

We note that, since the change of ν corresponds to the change of the driving frequency ω, LS $\chi(\omega)$ will take different values for different curves in Fig. 2. On the other hand, ϵ_1 depends on $\chi(\omega)$ [cf. Eq. (65a)], and, therefore, in order to keep ϵ_1 constant for different curves in the figure, one has to change the amplitude of the driving h_1. However, as will be shown below, for the relevant growth models, LS $\chi(\omega)$ is characterized by a smooth (nonexponential) form of the dispersion curve. This is in contrast to LS for escape of a Brownian particle,[26,30] which decays exponentially for large ω.

V. LOGARITHMIC SUSCEPTIBILITY FOR PARTICULAR MODELS OF NUCLEATION

For weak to moderately strong driving forces, the parameters of the dynamical model of nucleation enter the expression for the nucleation rate only in terms of the function $U(t)$ in Eq. (43), which is given by LS. For low-frequency driving, LS $\chi(\omega)$ is $\approx -g_0^*$, and then $U(t)=-g_0^*h(t)$. This corresponds to simple adiabatic modulation of the nucleation barrier (however, retardation effects can still be important, as discussed above). On the other hand, for high-frequency

driving, function $U(t)$ and the driving-force-induced change of the activation barrier $U^*=\min U(t)$ (for $|U^*|\gg D$) are determined by the frequency dispersion of $\chi(\omega)$.

We noted earlier that, for a given model, LS can be found by making the Fourier transform in Eq. (45) of the time-reversed speed at which the size of a subcritical nucleus decreases in the absence of fluctuations. This decrease is described by Eq. (8). We will analyze LS for the dynamical models which describe 2D layer-by-layer nucleation during overpotential deposition, and also nucleation of condensed monolayers in underpotential deposition. In both cases nucleation is characterized by small supersaturation, and relatively large sizes of critical nuclei can be expected.[11] Layer-by-layer nucleation occurs during deposition on native metal [e.g., in deposition of Ag on Ag (Refs. 11, 31) or Ag on Au (Ref. 32)] or in the case of small crystallographic overlayer-substrate misfit.

In 2D nucleation, the size g of a nucleus is proportional to its area, and the surface energy in Eq. (18) is proportional to the length of the boundary (which is assumed to be circular), so that in Eq. (18) $A(g)=\gamma g^{1/2}$. A few simple growth mechanisms are known in the literature. When diffusion on a surface is much slower than the attachment of ions from the solution to the surface, the ions are most likely attached to the nuclei directly from the electrolyte (direct transfer mechanism). In this case the rate at which ions are attached is proportional to the area of nucleus g,

$$a(g)=\sigma_{dt}g. \tag{87}$$

Using $a(g)$ and $A(g)$, we can explicitly find the optimal nucleation path from Eq. (37) and then obtain LS from Eq. (45),

$$g_0(t)=g_0^*(1-\exp[-\lambda^* t])^2, \quad \lambda^*=\frac{\sigma_{dt}\delta\mu_0}{2},$$
$$\chi(\omega)=g_0^* Y_{dt}\left(\frac{\omega}{\lambda^*}\right), \quad Y_{dt}(\nu)=-\frac{2}{(1-i\nu)(2-i\nu)}. \tag{88}$$

In the opposite case, where surface diffusion of adatoms is fast, whereas the activation barrier for transitions through the double layer is high, 2D nuclei grow by attaching adatoms from the surface rather than directly from the electrolyte. Such growth can be modeled in two simple ways. If, before an atom attaches to a nucleus, it had to ''hit'' the boundary of the nucleus (the step on the surface) several times, then the nuclei grow in the ''ballistic'' regime where the attachment rate $a(g)$ is proportional to the length of the boundary,

$$a(g)=\sigma_b g^{1/2}. \tag{89}$$

Using Eqs. (37) and (45), we can write the optimal nucleation path and the corresponding LS in the form

$$s(x)=-(x^{1/2}+\ln(1-x^{1/2})),$$
$$s=\lambda^* t, \quad x=g_0(t)/g_0^*, \quad \lambda^*=\frac{\sigma_b\delta\mu_0}{2(g_0^*)^{1/2}}, \tag{90}$$
$$\chi(\omega)\equiv g_0^* Y_b\left(\frac{\omega}{\lambda^*}\right), \quad Y_b(\nu)=-\int_0^1 dz\,\exp[i\nu s(z)]. \tag{91}$$

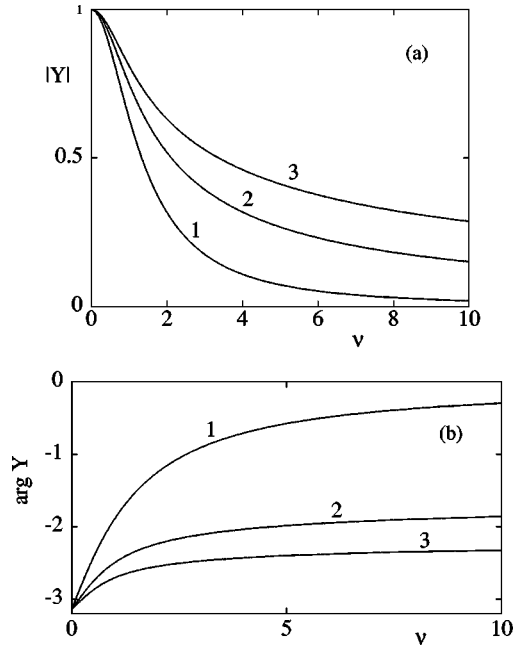

FIG. 3. Frequency dependence of the absolute value (a) and the phase (b) of logarithmic susceptibility, $\chi(\omega)=g_0^* Y(\omega/\lambda^*)$, for different nucleation models. Curves 1–3 correspond to the direct transfer model Eq. (88), the ballistic model Eq. (91), and the diffusion-limited model Eq. (95), respectively.

In particular, for large $\nu=\omega/\lambda^*$,

$$Y_b(\nu)\sim 2i\nu^{-1}, \quad \nu\to\infty. \tag{92}$$

On the other hand, if an adatom ''sticks'' to the nucleus once it has approached the nucleus boundary, the attachment rate $a(g)$ is determined by diffusion-limited growth and is independent of nucleus size in the 2D case,

$$a(g)=\sigma_{dl}. \tag{93}$$

Using Eqs. (37) and (45), we can write the optimal nucleation path and the corresponding LS in the form

$$s(x)=-(x^{1/2}+\tfrac{1}{2}x+\ln(1-x^{1/2})),$$
$$s=\lambda^* t, \quad x=g_0(t)/g_0^*, \quad \lambda^*=\frac{\sigma_{dl}\delta\mu_0}{2g_0^*}, \tag{94}$$
$$\chi(\omega)\equiv g_0^* Y_{dl}\left(\frac{\omega}{\lambda^*}\right), \quad Y_{dl}(\nu)=-\int_0^1 dz\,\exp[i\nu s(z)]. \tag{95}$$

In the limit of large $\nu=\omega/\lambda^*$

$$Y_{dl}(\nu)\approx\zeta\nu^{-2/3}, \quad \zeta=2\cdot 3^{-1/3}\Gamma^{-1}(1/3). \tag{96}$$

The frequency dependence of LS for the above nucleation models is plotted in Fig. 3(a) and 3(b).

The ballistic and diffusion-limited models of $a(g)$ can also be relevant for nucleation in underpotential deposition where a submonolayer, or one or two monolayers of a metal, grow on the cathode made from a different metal, with the potential which is positive with respect to the Nernstian equilibrium potential for bulk deposition. Nucleation in underpotential deposition corresponds to condensation of adatoms on the surface from a disordered low-coverage phase into ordered clusters.[33,11] The role of the ion transfer from the so-

lution is negligible during surface phase transformations because of the large activation barrier for the ions. Supersaturation $\delta\mu(t)$ in the case of underpotential deposition is the difference in chemical potentials of the atoms in the ordered clusters and in the disordered phase.

The above models correspond to simple limiting cases of surface growth. In the general case the growth law will be more complicated. We note, however, that instead of using particular dynamical models, LS can be determined experimentally by measuring the nucleation rate. In the simplest case one can use a monochromatic driving force and measure the driving-force-induced increment of the average nucleation rate, $A=\tilde{\mathcal{J}}/\mathcal{J}_0$. According to Eq. (65), this allows us to determine the absolute value of LS $|\chi(\omega)|$. The measurements can be performed in a broad range of driving force amplitudes, but the most advantageous regime corresponds to $\epsilon_1 \gg 1$ where the force affects the nucleation rate exponentially strongly, $A \gg 1$. By measuring the logarithm of A and using Eq. (65), one can find the change of the nucleation barrier D/ϵ_1 and therefore $|\chi(\omega)|$ at the driving frequency.

The frequency dependence of the phase of LS can be recovered by measuring the time-averaged nucleation rate for a nonsinusoidal periodic driving force. In the simplest case of a biharmonic driving force,

$$h(t)=\sum_{n=-2}^{n=2} h_n \exp(in\omega t), \quad h_{-n}=(h_n)^{\dagger},$$

the factor A, which shows the driving-force-induced increase of the average nucleation rate, is equal to

$$A=\frac{1}{2}\sum_{n=0}^{\infty} I_{2n}\left(\frac{1}{\epsilon_1}\right) I_n\left(\frac{1}{\epsilon_2}\right)\cos[n(\Phi+\Theta(\omega)+\pi)],$$

$$\Theta(\omega)=2\arg\chi(\omega)-\arg\chi(2\omega), \quad \Phi=2\arg h_1-\arg h_2, \tag{97}$$

$$\epsilon_k \equiv \frac{D}{2h_k|\chi(k\omega)|}, \quad k=1,2.$$

Here, we used Eq. (63) and the explicit form of the function $U(t)$ in Eq. (43). For strong driving, $\epsilon_n \ll 1$, Eq. (97) goes over into the asymptotic value of A in Eq. (64), with account taken of the explicit form of the driving-force-induced correction to the nucleation barrier U^*,

$$U^*=\min_{\varphi}\left[\frac{1}{\epsilon_1}\cos\varphi+\frac{1}{\epsilon_2}\cos(2\varphi-\Phi-\Theta(\omega))\right]. \tag{98}$$

The average nucleation rate Eq. (97) depends on the phase difference Φ between the harmonics of the driving force. For strong driving this dependence is exponentially strong and is determined by the variation of U^* with Φ. Plots of A vs Φ for different driving strengths are shown in Fig. 4. The amplitudes of the harmonics weighted with the appropriate absolute values of LS are chosen equal to each other, $\epsilon_1=\epsilon_2$, so that the effect of the interference between the harmonics is maximal. It is seen from Fig. 4 that, in the case of strong driving, the dependence of $\ln A$ on Φ is very sharp near the minima of A. In fact, the dependence of U^* on Φ is singular at the minima. This effect was analyzed in Ref. 20 and corresponds to the fact that function $U(t)$ may have two minima per period, and then U^* is determined by the global minimum of $U(t)$ [cf. Eq. (98)]. The relative depths of the minima depend on Φ, and for the values of Φ where the two minima have equal depths, the derivative of U^* with respect to Φ changes discontinuously. This singularity is smeared out by noise D, as seen in Fig. 4.

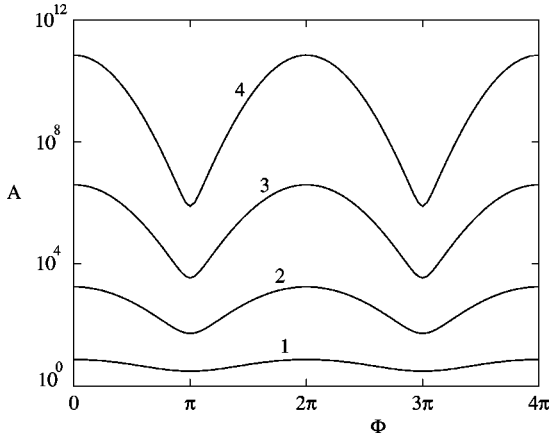

FIG. 4. Ratio A of the average nucleation rates with and without driving in Eq. (97) for a biharmonic driving force vs phase difference Φ between the harmonics. The reduced amplitudes of the harmonics are set equal to each other, $\epsilon_1=\epsilon_2$. Curves 1–4 correspond to $\epsilon_1=\epsilon_2=0.5$, 0.2, 0.11, 0.07.

We note that $\epsilon_{1,2}$ in Eqs. (97) and (98) depend on the absolute value of LS $|\chi(\omega)|$, which can be measured using a monochromatic driving force, as described above. Therefore the relative phase of LS $\Theta(\omega)$ can be recovered by measuring the dependence of A on Φ for different driving frequencies.

To find the phase of LS $\arg\chi(\omega)$ from $\Theta(\omega)$ one should solve the equation

$$2\arg\chi(\omega)-\arg\chi(2\omega)=\Theta(\omega). \tag{99}$$

We now discuss the boundary conditions for this equation. We note first of all that LS $\chi(\omega)$ approaches $-g_0^*$ as $\omega \to 0$, and therefore $\arg\chi(\omega)\to 0$ for $\omega\to 0$. For large ω, on the other hand, the asymptotic form of $\chi(\omega)$ is determined by the optimal nucleation path $g_0(t)$ for small-g, and $|\chi(\omega)|\to 0$ for $\omega\to\infty$, whereas $\arg\chi(\omega)$ approaches a finite constant value. Based on these boundary conditions, the solution of Eq. (99) can be written in two forms:

$$\arg\chi(\omega)=\omega t_0+\sum_{k=0}^{\infty} 2^{-k-1}\Theta(2^k\omega) \tag{100}$$

$$=\omega t_0-\sum_{k=0}^{\infty} 2^k\Theta(2^{-k-1}\omega), \tag{101}$$

which relate $\arg\chi(\omega)$ to the values of $\Theta(\Omega)$ with Ω being overtones $2^k\omega$ or subharmonics $2^{-k}\omega$ of frequency ω [in fact, the values of $\Theta(2^k\omega)$ for $k>0$ and $k<0$ are interrelated via Eq. (99)].

The first term in Eq. (101) identically satisfies Eq. (99) with arbitrary real t_0. The occurrence of this term is related to the time degeneracy of the unperturbed MPNPs $g_0(t-t_0)$, which was discussed earlier. We note that, due to

analyticity of $\chi(\omega)$ for $\omega\to 0$, the function $\Theta(\omega)$ is quadratic in ω for $\omega\to 0$, and therefore the second series for $\arg\chi(\omega)$ converges.

LS can also be found from measurements of the nucleation rate in the case of weak modulation where the harmonics of the nucleation current are linear in the amplitudes of the corresponding harmonics of the driving force,

$$\frac{j(g,t)}{\mathcal{J}_0}=1-D^{-1}\sum_n h_n\chi(\omega n)\Gamma\left(1+\frac{in\omega}{\lambda^*}\right)\times\exp[in\omega(t-\tau_0(g)-\tau_D)]. \tag{102}$$

Once LS is known, it is possible to find the nucleation current from Eq. (76) for any profile of the driving force without specifying the particular nucleation model, and this suggests how to perform the *learning control* of the nucleation process.

VI. THE FARADAY CURRENT

One of the standard ways to study the kinetics of the nucleation process in electrodeposition is to analyze the Faraday current in the electrochemical cell. Attachment to the cathode surface of an ion with the charge $-Ze$ contributes Z electrons to the Faraday current. In the case of small supersaturation, which is relevant to our analysis, the surface is close to equilibrium. In this case the elementary attachment/detachment processes to and from the surface, as well as fluctuational formation and collapse of small subcritical nuclei, give rise to zero-mean fluctuations of the current. After averaging over the time scale of elementary processes, the current density $i(t)$ is determined by the rate of formation and subsequent growth of supercritical nuclei. If supersaturation is created by a voltage pulse at $t=0$, and after that is held at a constant value $\delta\mu(t)=\delta\mu_0$, then in the steady state the current density $i_0(t)$ is proportional to the growth rate of the supercritical nuclei. The number of atoms in such nuclei $N_0(t)$ is equal to

$$N_0(t)=\int_0^t g(t-s)\mathcal{J}_0\,ds,\quad (g\gg g_0^*),\qquad i_0(t)=eZ\dot{N}_0(t)=eZg(t)\mathcal{J}_0. \tag{103}$$

Here, $\dot{g}=K_0(g)$ describes the deterministic growth of supercritical nuclei [cf. Eq. (76)]. Equation (103) corresponds to the qualitative picture in which supercritical nuclei emerge at a rate $\mathcal{J}_0$, which is independent of time for $t>0$. By time t the nuclei, which have emerged at instant s, will grow to size $g(t-s)$. Time t is chosen so that it largely exceeds the transient time, which is of the order of the reciprocal probability of creation of a critical nucleus in the system. For such t, the characteristic size of nuclei $g(t)$ is much larger than g_0^*.

In the case of periodic modulation of supersaturation $\delta\mu(t)$, the Faraday current density $i(t)$ has to be calculated taking into account the periodic modulation of the nucleation rate. Taking into account that the number of supercritical nuclei reaching size g_0^*+z over the time interval $(t,t+dt)$ is given by $j(g_0^*+z,t)$, we can write the expression for the current as

$$i(t)=eZ\int_0^t ds\dot{g}(t-s|z)j(g_0^*+z,s),\quad (g(t)\gg g_0^*), \tag{104}$$

where $g(0|z)\equiv g_0^*+z$, and the growth of supercritical nuclei $\dot{g}$ is calculated in the neglect of fluctuations. The value of z is limited by the condition that $z\ll g_0^*$, and in what follows we will assume that $z=z_D$ (the result is independent of the actual value of z).

We now investigate this expression for the models of nucleation considered above.

A. Current density for fast surface diffusion

In the diffusion-limited model of 2D nucleation, for large nuclei ($g\gg g_0^*$) the growth rate becomes independent of their size, $\dot{g}\approx 2\lambda^* g_0^*$. In this case the Faraday current in Eq. (104) is merely proportional to the integral over time of the periodic nucleation rate. At low modulation frequency $\omega/\lambda^*\ll 1$ the integral is reduced to the sum over the contributions from the vicinities of the maxima of nucleation rate $j(g_0^*+z_D,s)$ at $s=t_{\max}^n$ [see Eq. (78)] that correspond to the arrivals of the MPNPs to the critical region. In this limit one obtains

$$i(t)=2eZg_0^*\lambda^*\mathcal{J}_0TA\sum_{n=0}^{\infty}\theta(t-t_{\max}^n),\qquad i_0(t)\approx 2eZg_0^*\lambda^*\mathcal{J}_0 t,\quad (t\gg 1/\lambda^*). \tag{105}$$

Here, $\theta(x)$ is the step function, and the value of λ^* is given by Eq. (94).

The current Eq. (105) is approximately time independent in between the instants $t_{\max}^n$ and the increments by a constant when t goes through the next $t_{\max}^n$. After a long time has elapsed since the modulated overvoltage is turned on ($\omega t\gg 1$), so that many terms in the sum contribute to the current, the increments of the current at $t=t_{\max}^n$ are small compared to its magnitude, which is then determined by the average nucleation rate,

$$i(t)=Ai_0(t)\propto t,\quad (\omega t\gg 1).$$

We note that the above analysis for the Faraday current density applies to the initial state of nucleation when the surface fraction covered by the deposit is small.

For the ballistic model of nucleation, the growth of large nuclei is parabolic in time, $g=g_0^*(\lambda^* t)^2$ [cf. Eq. (90)]. Similar to the case of diffusion-limited nucleation after a long time has elapsed since the overpotential pulse is turned on, the time oscillations of the nucleation rate are averaged out, in the expression for Faraday current Eq. (104) at $\omega t\gg 1$ and the average current is determined by the average nucleation rate,

$$i(t)=Ai_0(t)=AeZ\mathcal{J}_0(\lambda^* t)^2,\quad (\omega t\gg 1). \tag{106}$$

B. Faraday current for the direct transfer model of nucleation

In the direct transfer model, the size of the nuclei grows in time exponentially [cf. Eq. (88)], and the Faraday current is mostly determined by the nuclei with the size close to the

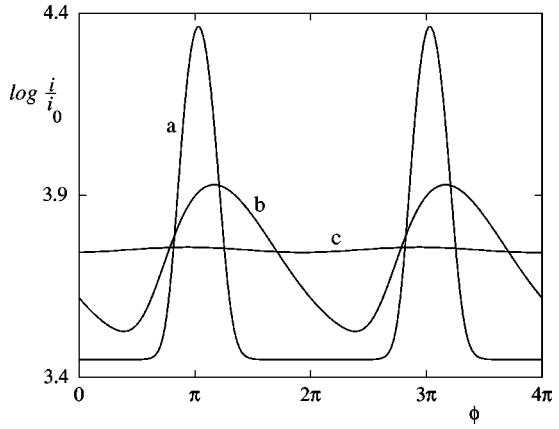

FIG. 5. Periodic oscillations of the ratio of the Faraday currents in the presence and in absence of ac modulation of the electrode potential calculated for the direct transfer nucleation model [the phase of the oscillations $\phi=\phi(t)$ is defined in Eq. (107)]. Curves a–c correspond to the reduced driving frequency $\nu=0.1$, 1, 3.14.

maximal, for given t. The expression for the current for monochromatic driving can be obtained from Eqs. (76) and (52), assuming that $g(t)\approx g^*\exp[2\lambda^* t]$ in Eq. (104),

$$\frac{i(t)}{i_0(t)}=\sum_n I_n\left(\frac{1}{\epsilon}\right)\frac{\Gamma(1-in\nu)}{1-in\nu/2}\exp[-in\varphi],$$

$$i_0(t)=eZ\mathcal{J}_0 g_0^*\exp[2\lambda^* t],\quad \varphi=\omega(t-\tau_D)+\arg Y_{dt}(\nu). \tag{107}$$

Here, $\Gamma(x)$ is a gamma function, λ^* and ν are defined in Eqs. (82) and (88), respectively. In Fig. 5 we show the dependence of ratio $i(t)/i_0(t)$ on time for different values of the reduced frequency $\nu=\omega/\lambda^*$. For small $\nu\ll 1$, ratio $i(t)/i_0(t)$ is a steep periodic function of time, and current $i(t)$ displays modulated exponential behavior. The local maxima of the current corresponds to the values of $t\approx t^n_{\max}$. When ν increases the modulation effect in $i(t)$ decreases and eventually disappears, and ratio $i(t)/i_0(t)\to A=I_0(1/\epsilon)$.

VII. CONCLUSIONS

In the present work we considered the steady-state nucleation rate in periodically driven systems where the driving force modulates in time the deviation of the chemical potential from the equilibrium value. Analysis was done for the case of the large size of a critical nucleus and was based on the solution of the Fokker–Planck equation (FPE) for the nuclei distribution function. In obtaining the nonequilibrium steady-state distribution of subcritical nuclei we relied on the underlying picture of large dynamical fluctuations and used the WKB-type technique to solve the FPE equation. In the vicinity of the critical state the asymptotic solution was matched with the solution of the linearized FPE. As a result we have obtained the nucleation rate in the closed analytical form in Eq. (76) which is a generalization of the Zeldovich formula for the case of periodically driven systems.

The result applies in the broad range of driving force strengths, from the linear regime where the Fourier harmonics of nucleation current $j(g,t)$ are linear in the force amplitude to the *logarithmically linear* regime, where the driving force affects $j(g,t)$ exponentially strongly, but $\ln j(g,t)$ is linear in the force amplitude. In both linear and logarithmically linear regimes (and in the whole intermediate range) the driving-force-induced change of $j(g,t)$ is described in terms of a certain spectral function $\chi(\omega)$ which we call logarithmic susceptibility (LS). Similar to standard linear susceptibility, $\chi(\omega)$ is determined by the dynamics of the system in the absence of external driving, but the crucial difference lies in the fact that $\chi(\omega)$ is determined by large dynamical fluctuations of the system away from the steady state and depends on the global properties of the evolution of the system along the most probable nucleation path (MPNP). The explicit form of $\chi(\omega)$ is determined by the model of nucleation.

In the case of monochromatic driving, the nucleation current is determined by the absolute value of LS, $|\chi(\omega)|$, whereas for the driving force with several harmonics both the amplitudes and phases of $\chi(\omega)$ are important. We investigated the average nucleation rate in the presence of biharmonic driving for various driving force strengths and have shown that, in the limit of relatively strong driving, the effective nucleation barrier displays singular behavior as a function of the relative phase Φ between the force harmonics. The singularity is smeared out on the scale $\delta\Phi\propto k_BT/h_n\chi(n\omega)$ (where $n=1,2$, and T is temperature). We have shown how the phase of LS $\arg\chi(\omega)$ can be obtained from measurements of the average nucleation rate as a function of Φ for different ω.

Equation (76) describes nucleation for the entire range of driving force frequencies from small (the adiabatic driving) to high, where the driving is strongly nonadiabatic. The modulation in time of the nucleation rate is exponentially strong for low-frequency driving. Here, nucleation is most likely to occur where the nucleation barrier is at its minimum. For larger driving frequencies the nuclei that have approached critical size will remain in the critical region for a time longer than the force period. This gives rise to rectification of the nucleation rate. The nonzero Fourier harmonics of the nucleation current $\propto\exp[-n\omega\pi/2\lambda^*]$, where λ^* is an eigenvalue that describes the dynamics of the nuclei in the vicinity of the critical state.

It is important to emphasize that a high-frequency force can still *exponentially* strongly affect the nucleation rate, provided the force amplitude weighted with LS exceeds k_BT. In this case the MPNPs are synchronized with the phase of the driving force, and $\ln j(g,t)$ is proportional to the *thermodynamic work* [cf. Eq. (38)] done by the driving force during the formation of the critical nucleus. Thus $\ln j(g,t)$ is linear in the amplitude of the nonadiabatic driving force. However, for very high driving frequencies, $\omega\gg\lambda^*$. LS becomes small (it decays as a power of ω^{-1} for large ω). Then the driving-force-induced correction to the average nucleation rate is quadratic in the driving force amplitude.

Electrochemical systems are advantageous for studying effects of ac driving on nucleation rate because of the possibility to change supersaturation in a well-controlled way for by varying the electrode potential, without causing environmental changes and dissipative energy transfer. The frequency dispersion of LS is highly sensitive to the underlying nucleation mechanism. Measurements of LS allow creation of optimal driving force profiles for selective control of

nucleation kinetics, for example, for controlling 2D layer-by-layer nucleation mode at maximum growth rate.

Generally, LS $\chi(\omega)$ is a *nonanalytic* function of the frequency ω. This nonanalyticity arises in spite of the expression for $\chi(\omega)$ being of the causal form familiar from the theory of linear susceptibility in statistical physics. It is due to nonanalytic dependence of the nucleus size $g(t)$ on time for small-g (in the absence of driving and fluctuations). Respectively, the nonanalyticity of $\chi(\omega)$ arises for large ω. We have calculated $\chi(\omega)$ for the models of 2D nucleation in electrochemical deposition on a metal electrode. The following models of attachment of ions to the nucleus were discussed: (i) direct transfer from the electrolyte; (ii) surface diffusion with multiple reflection from a nucleus; and (iii) surface diffusion where ions stick to a nucleus once they reach it.

In conclusion we make estimates for a specific electrochemical system, $Ag(hkl)/AgNO_3$. This is an example of deposition on a native metal, and the critical nuclei are two dimensional. The growth of silver on one of the close-packed $Ag(hkl)$ single crystal faces from an aqueous solution containing Ag^+ has been experimentally studied in a number of papers (see Ref. 11 and references therein). In these studies techniques were developed for growing crystal faces with very low density of defects and no screw dislocations, and a detailed study of the kinetics of 2D nucleation (at constant overvoltage) on quasi-perfect crystal faces was performed. In particular, it was found that, at room temperatures, the transient time τ^* is of the order of several milliseconds. At small supersaturation, $\eta=7$ mV, the size of the critical nucleus g_0^* was estimated to be ~ 80, and the height of the nucleation barrier $\Phi_0^*\sim 10^{-19}$ J. At room temperature $\Phi_0^*/k_BT\sim 25$ and supersaturation $\delta\mu_0\sim 0.2k_BT$. Thus it is possible to use the continuous FPE for the nuclei distribution function and apply the large fluctuation theory to the analysis of nucleation, as it was done in the present paper. The data on the transients of the Faraday current in potentiostatic experiments indicate[11] that the current increases quadratically with time at the initial stage of nucleation. This suggests that the ballistic model of nucleation in Eq. (89) can apply. Using the amplitude of the overvoltage modulation $\sim 2-3$ mV, and keeping the dc value of $\eta\sim 6-7$ mV it may be possible to produce an exponentially strong modulation of the nucleation rate (by a factor $\sim\exp[-(6\div 10)]$). For stronger modulation of supersaturation, the numerical evaluation of the nucleation rates (to logarithmic accuracy) can be done based on the nonperturbative expression Eq. (33).

ACKNOWLEDGMENT

M.I.D. acknowledges financial support from the NSF funded MRSEC—Center for Sensor Materials at Michigan State University.

[1] (a) Ya. B. Zeldovich, Acta Physicochim. URSS **18**, 1 (1943); (b) J. Frenkel, *Kinctic Theory of Liquids* (Oxford University, Oxford, 1946).
[2] J. D. Gunton, M. San Miguel, and P. S. Sahni, in *Phase Transitions and Critical Phenomena*, edited by C. Domb and J. L. Lebowitz (Academic, New York, 1983), Vol. 8, p. 267.
[3] J. S. Langer, in *Solids Far From Equilibrium*, edited by C. Godreche (Cambridge University Press, Cambridge, 1992), p. 297.
[4] J. Feder, K. C. Russell, J. Lothe, and G. M. Pound, Adv. Phys. **15**, 111 (1966); K. Binder and D. Stauffer, *ibid.* **25**, 343 (1976); K. F. Kelton, A. L. Greer, and C. V. Thompson, J. Chem. Phys. **79**, 6261 (1983); L. Demeio and B. Shizgal, *ibid.* **98**, 5713 (1993).
[5] V. A. Shneidman and M. C. Weinberg, J. Chem. Phys. **97**, 3621 (1992).
[6] H. Kumomi and T. Yonehara, J. Appl. Phys. **75**, 2884 (1994).
[7] J. Vereecken and R. Winand, Electrochim. Acta **22**, 401 (1977); R. Wiart, *ibid.* **35**, 1587 (1990); Z. Stoynov, B. Grafov, B. Savova-Stoynov, and V. Elkin, *Electrochemical Impedance* (Nauka, Moscow, 1991).
[8] C. Livermore and P. Wong, Phys. Rev. Lett. **72**, 3847 (1994).
[9] S. A. Perusich and R. C. Alkire, J. Electrochem. Soc. **138**, 700 (1991); **138**, 708 (1991).
[10] V. N. Smelyanskiy, M. I. Dykman, H. Rabitz, and B. E. Vugmeister, Phys. Rev. Lett. **79**, 3113 (1997).
[11] E. Budevski, G. Staikov, and W. J. Lorenz, *Electrochemical Phase Formation and Growth* (VCH, Weinheim, New York, 1996), p. 205.
[12] H. A. Kramers, Physica (Utrecht) **7**, 284 (1940).
[13] V. A. Shneidman and P. Hanggi, Phys. Rev. E **49**, 641 (1994).
[14] M. I. Freidlin and A. D. Wentzell, *Random Perturbations of Dynamical Systems* (Springer-Verlag, New York, 1984).
[15] M. I. Dykman and M. A. Krivoglaz, in *Soviet Physics Reviews*, edited by I. M. Khalatnikov (Harwood, New York, 1984), Vol. 5, p. 265.
[16] R. Graham, in *Noise in Nonlinear Dynamical Systems*, edited by F. Moss and P. V. E. McClintock (Cambridge University Press, Cambridge, 1989), p. 225.
[17] M. I. Dykman, Phys. Rev. A **42**, 2020 (1990); S. J. B. Einchcomb and A. J. McKane, Phys. Rev. E **51**, 2974 (1995).
[18] R. S. Maier and D. L. Stein, Phys. Rev. Lett. **71**, 1783 (1993); Phys. Rev. E **48**, 931 (1993); J. Stat. Phys. **83**, 291 (1996).
[19] (a) M. I. Dykman, M. M. Millonas, and V. N. Smelyanskiy, Phys. Lett. A **195**, 53 (1994); (b) V. N. Smelyanskiy, M. I. Dykman, and R. S. Maier, Phys. Rev. E **55**, 2369 (1997).
[20] M. I. Dykman, H. Rabitz, V. N. Smelyanskiy, and B. E. Vugmeister, Phys. Rev. Lett. **79**, 1178 (1997).
[21] (a) R. Graham and T. Tél, Phys. Rev. Lett. **52**, 9 (1984); (b) R. Graham and T. Tél, J. Stat. Phys. **35**, 729 (1984); (c) R. Graham and T. Tél, Phys. Rev. A **31**, 1109 (1985).
[22] (a) M. I. Dykman, D. G. Luchinsky, P. V. E. McClintock, and V. N. Smelyanskiy, Phys. Rev. Lett. **77**, 5229 (1996); (b) D. G. Luchinsky and P. V. E. McClintock, Nature (London) **389**, 463 (1997).
[23] M. I. Dykman, V. N. Smelyanskiy, T. Takexiko, and J. Ross (unpublished).
[24] M. I. Dykman, E. Mori, J. Ross, P. M. Hunt, J. Chem. Phys. **100**, 5735 (1994); M. I. Dykman, V. N. Smelyanskiy, R. S. Maier, and M. Silverstien, *ibid.* **100**, 19197 (1996).
[25] L. D. Landau and E. M. Lifshitz, *Mechanics* (Pergamon, London, 1976).
[26] V. N. Smelyanskiy, M. I. Dykman, and B. Golding, Phys. Rev. Lett. **82**, 3193 (1999).
[27] T. Naeh, M. M. Klosek, B. J. Matkowsky, and Z. Schuss, SIAM (Soc. Ind. Appl. Math.) J. Appl. Math. **50**, 595 (1990); P. Talkner, Z. Phys. B **68**, 201 (1987).
[28] See M. Marder, Phys. Rev. Lett. **74**, 4547 (1995), and references therein.
[29] M. Abramowitz and I. A. Stegun, *Handbook of Mathematical Functions* (Dover, New York, 1970).
[30] M. I. Dykman, D. G. Luchinskiy, R. Mannella, P. V. E. McClintock, and V. N. Smelyanskiy (unpublished).
[31] J. Vrijmoeth, H. A. van der Vegt, J. A. Meyer, E. Vlieg, and R. J. Behm, Phys. Rev. Lett. **72**, 3843 (1994).
[32] S. G. Corcoran, G. S. Chakarova, and K. Sieradzki, Phys. Rev. Lett. **71**, 1585 (1993).
[33] M. F. Toney, J. N. Howard, J. Richer, *et al.*, Phys. Rev. Lett. **75**, 4473 (1995); J. Zhang, Y.-E. Sung, P. A. Rikvold, *et al.* J. Chem. Phys. **104**, 5699 (1996); B. M. Ocko, O. M. Magnussen, J. X. Wang, *et al.*, Physica B **221**, 238 (1996); U. Schmidt, S. Vinzelberg, G. Staikov, ''Pb UPD on Ag(100) and Au(100)—2D phase formation studied by *in situ* STM,'' Pop. Sci. (U.S.) **348**, 261 (1996); B. M. Ocko, J. X. Wang, and T. Wandlowski, Phys. Rev. Lett. **79**, 1511 (1997).